UPPSALA
UNIVERSITET

UPTEC X 16 012
Examensarbete 30 hp
Oktober 2016

Obesogenic molecules breaching Caco-2 cells: intracellular regulation of tight junctions

Tim Hagelby Edström

UPPSALA UNIVERSITET

Degree Project in Molecular Biotechnology

Masters Programme in Molecular Biotechnology Engineering,
Uppsala University School of Engineering

UPTEC X 16 012	**Date of issue 2016-10**

Author

Tim Hagelby Edström

Title (English)

Obesogenic molecules breaching Caco-2 cells: intracellular regulation of tight junctions

Title (Swedish)

Abstract

Impaired function of the human intestinal epithelial barrier (IEB) might allow for permeability of harmful substances, such as obesogens, which induce obesity and further implications. Tight junction (TJ) proteins are the key component for normal functions of the barrier. In this master thesis, the correlation between increased TJ permeability of the IEB and absorption of obesogens was studied. The effect of obesogens on TJ expression was also investigated. Permeability tests performed on Caco-2 cell monolayers exposed to obesogens showed altered permeability, indicating that obesogens might have an effect on TJ protein expression. Furthermore, impaired monolayers showed increased permeability, which implies that impaired functions of IEB lead to increased absorption of obesogens.

Keywords

Obesogens, tight junctions, permeability, intestinal barrier, Caco-2 cell

Supervisors

Dominic-Luc Webb
Uppsala University

Scientific reviewer

Thomas Lind
Uppsala University

Project name	Sponsors
Language **English**	Security
ISSN 1401-2138	Classification
Supplementary bibliographical information	Pages **42**

Biology Education Centre Biomedical Center Husargatan 3, Uppsala
Box 592, S-751 24 Uppsala Tel +46 (0)18 4710000 Fax +46 (0)18 471 4687

Obesogenic molecules breaching Caco-2 cells: intracellular regulation of tight junctions

Tim Hagelby Edström

Populärvetenskaplig sammanfattning

Epitelet i tarmkanalen fungerar som en selektiv barriär som underlättar absorption av väsentliga joner och molekyler. Nedsatt funktion av denna barriär kan leda till att även skadliga ämnen transporteras genom tarmväggen. I bland annat plast och färg finns det så kallade obesogener, vilka kan orsaka fetma och påverka epitelets permeabilitet om de tas upp av kroppen. Ökad permeabilitet är associerad med sjukdomar såsom irriterad tarm och koloncancer. I dagsläget finns det ingen klar bild av hur detta fungerar i detalj.

Målet med det här projektarebetet var att studera hur obesogener tas upp av tarmcellerna och hur detta kan påverka permebiliteten. Under projektets gång utsattes mänskliga celler för olika obesogener, varpå cellerna studerades för att se ifall barriärfunktionen ändrats. Resultaten kan förhoppningsvis bidra till mer kunskap i ämnet och vara till nytta för framtida studier av obesogener och deras skadliga påverkan.

Examensarbete 30 hp

Civilingenjörsprogrammet i Molekylär bioteknik

Uppsala universitet, oktober 2016

Table of Contents

List of abbreviations

4,4'oBBV	1,1'-bis(2-boronobenzyl)-4,4'-bipyridinium
BPA	Bisphenol A
BPA AF	Bisphenol AF
BSA	Bovine serum albumin
DMEM-PEST	Dulbecco's modified eagle medium-penicillin/streptomycin solution
DMSO	Dimetylsulfoxid
DPBS(-)	Dulbecco's phosphate-buffered saline without calcium and magnesium
ECL	Enhanced chemiluminescent
EDTA	Ethylenediaminetetraacetic acid
ER-β	Estrogen receptor beta
FA_{cum}	Cumulative fraction transported
GAPDH	Glyceraldehyde 3-phosphate dehydrogenase
HBSS(-)	Hank's balanced salt solution without calcium and magnesium
HBSS(+)	Hank's balanced salt solution with calcium and magnesium
HEPES	4-(2-hydroxyethyl)-1-piperazineethanesulfonic acid
HPTS	8-hydroxypyrene-1,3,6-trisulfonic acid
HRP	Horseradish Peroxidase
IBD	Inflammatory bowel disease
IBS	Irritable bowel syndrome
IEB	Intestinal epithelial barrier
Imi	Imidacloprid
JAM	Junction adhesion molecule
P_{app}	Apparent permeability coefficient
PBS	Phosphate-buffered saline
PPAR-γ	Proliferator-activated receptor gamma
PVDF	Polyvinylidene difluoride
RCF	Relative centrifugal force
RIPA	Radioimmunoprecipitation assay
SDS	Sodium dodecyl sulfate
SDS-PAGE	SDS-polyakrylamidelektrofores
SEM	Standard error of the mean
TBST	Tris-Buffered Saline and Tween 20
TBT-Cl	Tributyltin chloride
TEER	Transepithelial electrical resistance
TJ	Tight junction
TRIS base	2-Amino-2-(hydroxymethyl)-1,3-propanediol
WB	Western blot
ZO	Zona occuldens

1. Introduction

1.1 Background

The epithelium of the human intestinal epithelial barrier (IEB) tract acts as a selective barrier that facilitates absorption of essential ions and molecules while protecting against harmful substances. This barrier is constituted by four types of intercellular junctions; desmosomes, adherens junctions, gap junctions and tight junctions (TJs) [1]. The TJs are located closest to the lumen where they seal and control the paracellular pathway of transport from the apical to the basolateral side of the epithelium [2]. The TJ complex consists of integral membrane proteins such as claudins and junctional adhesion molecules (JAMs), and peripheral membrane proteins such as zonula occludens (ZOs) [1].

Dysfunctional distribution and expression of TJs have been linked to impaired paracellular barrier function, consequently inducing an increased paracellular permeability of the intestinal epithelium. Increased permeability is associated with diseases such as inflammatory bowel disease (IBD), irritable bowel syndrome (IBS), celiac disease, colon cancer and type 2 diabetes [3]. Clinical studies have shown that patients with IBS have decreased expression of TJ proteins such as occludin, JAM-A and several sealing claudins, while having increased expression of pore-forming claudin-2 [4]. Furthermore, increased permeability might allow for permeation of harmful substances, such as obesogens, through the epithelium.

1.1.1 Obesogens

Obesogens are xenobiotics that can promote lipid accumulation and adipogenesis, which can lead to obesity. Most obesogens are endocrine disrupting chemicals as they can mimic natural lipophilic hormones or inhibit the metabolism of endogenous steroid hormones [5]. There are several obeseogens present in the environment, such as bisphenol A (BPA), tributyltin chloride (TBT-Cl) and imidacloprid (Imi). The chemically produced BPA is used by the industry to produce plastics, e.g. water bottles, and epoxy resin, e.g. lining in food cans. TBT-Cl is used in anti-fouling paint for watercrafts [5], while Imi is used as an insecticide in agriculture [6]. These obesogens leak into the environment and are ingested by humans [5, 7].

1.1.2 Obesogen pathways

Obesogens can act on several and complex intracellular molecules [8]. BPA has been shown to bind to the oestrogen receptor beta (ER-β), which is a nuclear receptor for oestrogen that upon binding acts on gene transcription [8, 9]. When oestradiol binds to ER-β, it can upregulate JAM-A in the Caco-2 cell line [10], and it has been shown that BPA may act in the same way [7]. This suggests that BPA can affect TJs, particularly JAM-A, and alter the paracellular permeability. Furthermore, BPA has been shown to promote human adipocyte differentiation by upregulating the expression of peroxisome proliferator–activated receptor gamma (PPAR-γ) [11]. Similarly, Imi and TBT-Cl have also been shown to induce adipocyte differentiation and lipid accumulation by acting on PPAR-γ [6, 12].

Moreover, PPAR-γ has also been linked to regulation of TJs, as the PPAR-γ agonist troglitazone can reduce human colonic paracellular permeability, probably by inducing cell differentiation and consequently increasing the amount of TJ proteins [13]. In contrast, the PPAR-γ agonist rosiglitazone has been reported to decrease the expression of ZO-1 in mice colon [14]. In addition, both agonists have been shown to increase expression of claudin-1 and claudin-4 in human nasal epithelial cells [15], which suggests that they may affect claudin-2 as well. Adding further complexity to the mechanism is that it has also been shown that TBT-Cl can inhibit the activity of human placental aromatase cytochrome P450, which catalyses the conversion of androgens to oestrogens [16]. The inhibition of aromatase activity can be linked to decreased levels of oestrogen and thus downregulation of oestrogen receptor target genes [5]. Hence, it is reasonable to believe that the expression of TJ proteins could be affected. In

summary, obesogens have been reported to act on multiple pathways to interfere with the endocrine system, consequently affecting the expression of TJ proteins (Fig. 1).

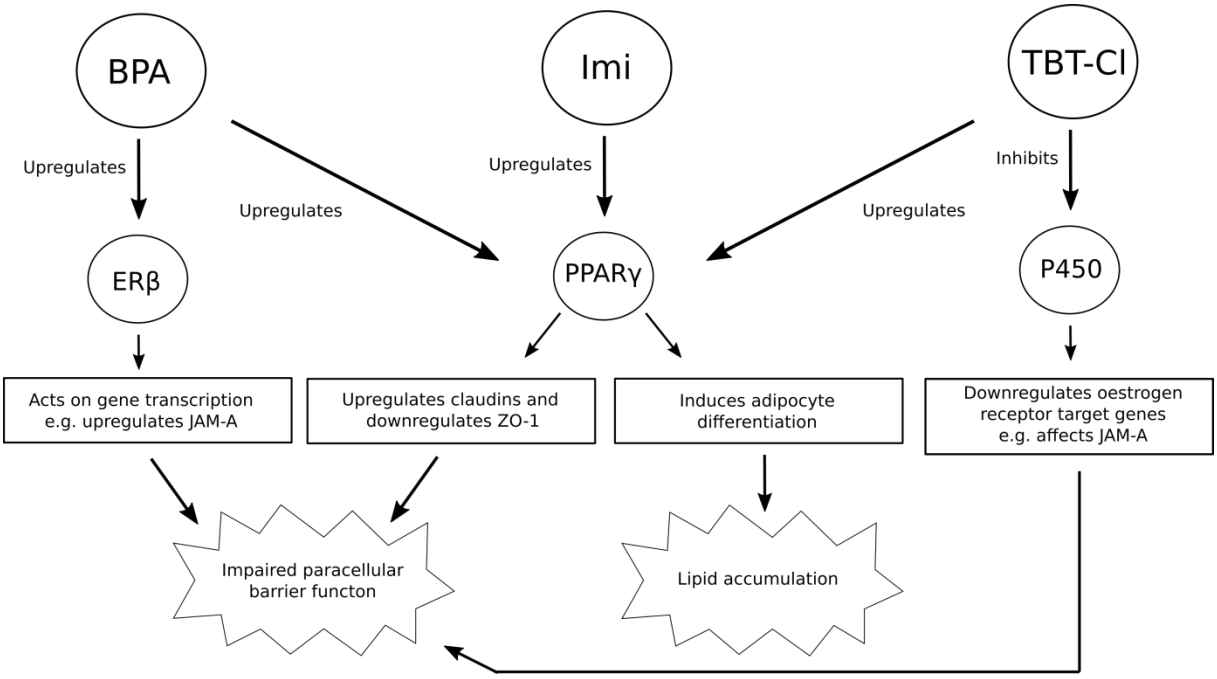

Figure 1. Pathways for obesogen regulation of TJ protein expression.

1.1.3 Epigenetic effect of obesogens

Obesogens might have an epigenetic effect, which means that they may induce heritable change in gene expression or the phenotype of a cell. Proposed mechanisms for this effect includes DNA methylation, modification of histone proteins and alteration of small and non-coding RNA expression levels. BPA has been shown to have epigenetic effect through these mechanisms in various mammals [17]. Hence, it is likely that the obesogens effect on the expression of TJ proteins may also be induced through epigenetic mechanisms.

1.2 Project aims and objectives

The aim of this project was to study if there is a correlation between increased TJ permeability of the intestinal epithelium and absorption of obesogens. Additionally, as obesogens act on intracellular signalling that affect gene expression, a related hypothesis that was tested is if obesogens alter the expression of intestinal TJs. To test these theories, four structurally unrelated endocrine disruptor molecules with convergent obesogenic action were studied: BPA, bisphenol AF (BPAF), TBT-Cl and Imi (Fig. 2). BPAF was included to investigate if the level of hydrophobicity affects the permeability of bisphenols. As outlined above, obesogens have multiple pathways to induce change in TJ expression, but the hypothesis for this study was that they individually act on single pathways. These actions were as following; BPA/BPAF acting on ER-β, Imi acting on PPAR-γ and TBT-Cl acting on aromatase cytochrome P450. This could result in a better understanding of how and why they have convergent physiological actions. In addition, epigenetic effects of obesogens on the expression of TJ proteins were studied.

Caco-2 cell culture was used as an *in vitro* gastrointestinal mucosa. Since these cells form a monolayer and express TJ proteins whilst growing on filters they are often used for transport studies [18], hence

making them suitable as a model of intestinal absorption. The permeability of the Caco-2 cell monolayer was studied using D-mannitol and lactulose as permeability markers. D-mannitol was assayed with an organoborane based sugar sensor coupled to a fluorophore. Lactulose was assayed using HPLC. The expression of TJ proteins in Caco-2 cells were studied using western blot (WB).

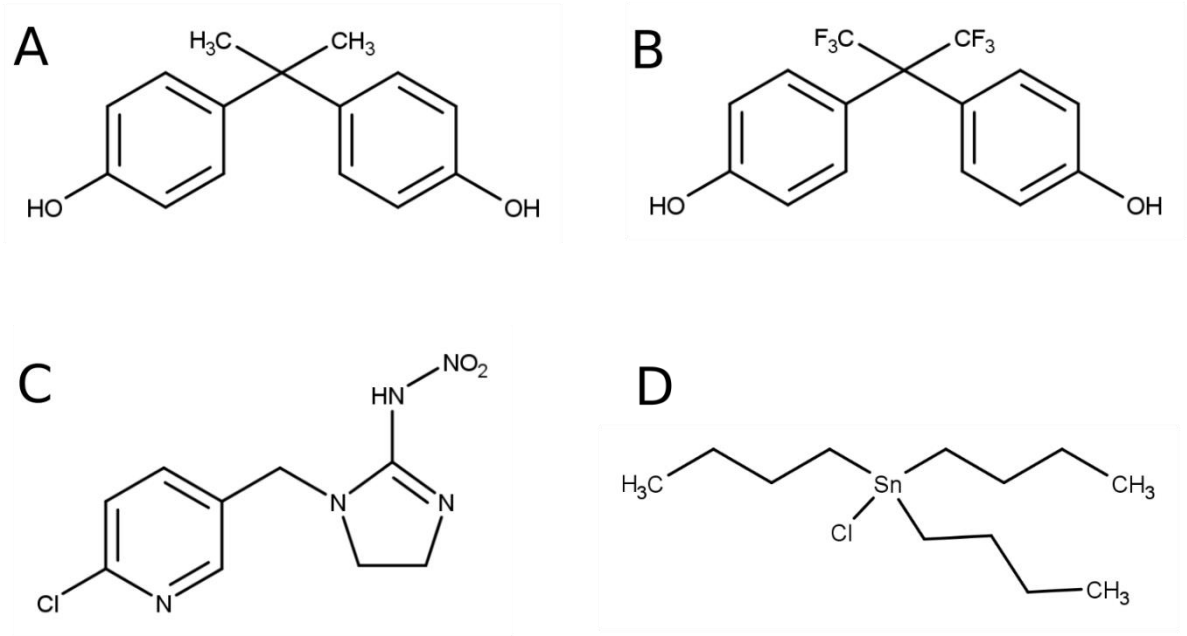

Figure 2. Chemical structure of (A) BPA, (B) BPAF, (C) Imi and (D) TBT-Cl. Note that the molecular sizes are comparable to a disaccharide, such as the permeability probe lactulose.

2. Methods

2.1 Permeability test on obesogen exposed Caco-2 cells using D-mannitol

2.1.1 Caco-2 cell culture and seeding

Caco-2 cells from passage number 102 (P-102) were cultured in a 75 cm^2 cell flask, with culture medium DMEM-PEST consisting of 500 mL Dulbecco's modified eagle medium (DMEM) high glucose (4500 mg/L glucose) with L-glutamine (without pyruvate), 50 mL Gibco® heat inactivated foetal bovine serum, 5 mL Gibco® minimum essential medium non-essential amino acids (100X) and 2.5 mL penicillin (20000 u/mL) - streptomycin (20 000 µg/mL) (PEST) solution (100X). When the cell monolayer was about 90 % confluent (after approximately 7 days), the cells were rinsed with Dulbecco's phosphate-buffered saline without calcium and magnesium (DPBS(-)). The cells were released with trypsin-EDTA solution consisting of 40 mL DPBS(-), 5 mL ethylenediaminetetraacetic acid (EDTA) and 5 mL Gibco® 2.5% trypsin (10X). Approximately 1 mL trypsin-EDTA solution was added and the flask was incubated (closed) for about 15 min, with in between knocking of flask. Trypsination was stopped by adding DMEM-PEST. The cells were re-suspended and counted using a Scepter™ 2.0 handheld automated cell counter. The cells were spun down for 5 min at 400 relative centrifugal force (RCF) and re-suspended in DMEM-PEST to a final concentration of 1 x 10^6 cells/mL. Cells were seeded on the apical side of a Millicell® 24-well cell culture plate at a density of 45 000 cells/well. DMEM-PEST medium was added to 400 µL at the apical side followed by 800 µL to the basolateral side. Culture medium was changed every second day for 21 days.

2.1.2 Exposing Caco-2 cell to obesogens

BPA, BPAF, Imi and TBT- Cl were separately dissolved in dimetylsulfoxid (DMSO) and diluted in DMEM-PEST to final concentrations of 10^{-10}, 10^{-9}, 10^{-8}, 10^{-7} and 10^{-6} M. Four hundred µL of respective obesogen solutions were added to separate wells on the apical side of the seeded cell culture plates. This was done in replicates of two wells per obesogen mixture. As a negative control, 1 % DMSO in DMEM-PEST was loaded in triplicates for the Imi/TBT-Cl plate and in quadruplets for the BPA/BPAF plate. Eight hundred µL DMEM-PEST was added to the basolateral side of each well. The plate was incubated for 24 h at 37 °C, 10 % CO_2 and humidified atmosphere.

2.1.3 D-mannitol transport test

The culture medium (containing obesogens) was removed after 24 h and the monolayers were washed twice with Hank's balanced salt solution without calcium and magnesium (HBSS(-)) (pH 7.4) for 15 min in incubator. D-mannitol (182.17 g/mol) was dissolved in water and diluted in HBSS(-) to a final concentration of 2 mM. Five hundred and fifty µL of the HBSS(-) and D-mannitol (2 mM) solution was added to the apical side. Eight hundred µL of HBSS(-) was added to the basolateral side. One hundred and fifty µL aliquots were immediately collected from the apical side and the plate was put in an incubator. The plate was manually shaken for a couple of seconds at 6 min intervals. After 30 minutes, 400 µL was collected from basolateral side on Imi and TBT-Cl plate, while 450 µL for the BPA and BPAF plates. Fresh HBSS(-) replaced the collected sample volume. The plates were once again put in incubator with manual shakings every 6 min. After 60 minutes, 150 µL apical samples and 400 µL (Imi and TBT-Cl)/450 µL (BPA and BPAF) basolateral samples were collected. The monolayers were washed with phosphate-buffered saline (PBS) and the plates were stored at -20 °C.

2.1.4 D-mannitol concentration determination

D-mannitol was assayed with the sugar sensor boronic acid-appended viologen 1,1'-bis(2-boronobenzyl)-4,4'-bipyridinium (4,4'oBBV), coupled to the fluorophore 8-hydroxypyrene-1,3,6-trisulfonic acid (HPTS) [19]. A 4X 4,4'oBBV fluorophore mix was prepared by dissolving 0.936

mg/mL of 4,4'oBBV (585 g/mol) in a 4x buffer containing 0.1 M monosodium phosphate (119.98 g/mol) 0.3117 % w/v and 0.1 M 4-(2-hydroxyethyl)-1-piperazineethanesulfonic acid (HEPES) (238.3 g/mol) 2.38 % w/v. The mix was vortexed and sonicated until dissolved. HPTS was added to the mix reaching a concentration of 4 µM. The mix was vortexed and sonicated. D-mannitol standards were prepared by 3X serial dilution from 20 mM (0.00364 g/mL) in the buffer mentioned above (diluted to 1x in water). Ten µL of the 4X 4,4'oBBV fluorophore mix was pipetted to each well on Corning® 3694 solid black half area plates. Thirty µL of collected samples, standards and blanks were added in quadruplets. The blanks were 1X buffer for standards and HBSS(-) with 1% DMSO for the samples. The plates were incubated on a plate shaker for 1 h at room temperature. The plates were then centrifuged at 2500 RCF for 11 min at 4 °C. The fluorescence was measured at 404/535 nm using a Tecan infinite M200 pro plate reader. Best fit for the standard curve was obtained by non-linear regression analysis by modelling the data with the four parameter logistic equation:

$$y = min + \frac{max - min}{1 + \frac{x^{-Hillslope}}{EC50}} \quad \text{[Eq. 1]}$$

Where *min* is the bottom and *max* is the top of the curve. Half maximal effective concentration (*EC50*) is the *x*-value for the curve half way between max and min. *Hillslope* is the slope at the midpoint of the curve. The analysis was performed in the scientific data analysis and graphing software SigmaPlot. The data obtained from standards on BPA and BPAF plates were used to model the curve as these did not seem to have signs of contaminations. The resulting standard curve was used for D-mannitol concentration determination.

2.1.5 Analysis of D-mannitol transport

Two replicate samples from the different obesogen exposed cells were compared to two randomly selected control wells per plate (two for the BPA/BPAF plate and two for the Imi/TBT-Cl plate). Furhter, the mass of D-mannitol was calculated at each specific sampling point for each sample. This was done by deriving the mass from the concentrations determined with the standard curve. The average mass and the standard error of the mean (SEM) was calculated from the derived masses. The resulting average mass and SEM was plotted in SigmaPlot. Further, the total mass of permeated D-mannitol was calculated by adding the mass in basolateral side at 60 min with the removed mass in basolateral at 30 min. The values were plotted together with the apical concentration at 30 min. Finally, an approximation of the percentage permeated mass of D-mannitol was made by calculating the fraction between the mass in basolateral side at 30 min and the apical side at 0 min. The resulting plot of these values was used to evaluate if respective obesogen altered the permeability across Caco-2 cell monolayers.

2.1.6 The apparent permeability coefficient for sucralose/D-mannitol transport

To evaluate the transport of the permeability markers D-mannitol and sucralose, the apparent permeability coefficient (P_{app}) and the cumulative fraction transported (FA_{cum}) were analysed and described accordingly to previous protocols [20]. P_{app} is used to describe rate (cm/s) of the analyte transport across the monolayer and FA_{cum} is viewed as a weighted normalised cumulative amount of the transported analyte. P_{app} was determined by first calculating FA_{cum}. The relation between P_{app} and FA_{cum} is defined as following:

$$FA_{cum} = \frac{1}{A} \times \sum_{k=1}^{i} \frac{[C_R(t_k) - f \times C_R(t_{k-1})] \times V_R}{[C_D(t_{k-1}) + C_D(t_k)]} = P_{app} \times t_i \quad \text{[Eq. 2]}$$

Where A denote monolayer surface area (cm^2), and the variables C_R and C_D denote concentrations (µM) in receiver (basolateral) side and donor (apical) side respectively. For the sampling intervals (i), t_k represents the time point (sec) at each sampling occasion (k), thus $C_R(t_k)$ denotes sample concentration at that sampling occasion. Factor f denotes sampling replacement factor, which is equal to $1 - V_S/V_R$, were V_S and V_R denote the volumes (cm^3) of sample and receiver respectively. Furthermore, P_{app} could be solved as the slope of FA_{cum} which was described in the protocol. Calculation of P_{app} can only be applied if diffusion occur during sink condition, which is satisfied when backwards diffusion (in this case basolateral to apical) is <10 % of donor concentration at each sampling occasion. According to protocol, P_{app} could be determined under non-sink conditions by nonlinear curve fitting of the following equation:

$$C_R(t) = \frac{M}{V_D + V_R} + (C_{R,0} - \frac{M}{V_D + V_R})e^{-P_{app}A\left(\frac{1}{V_D}+\frac{1}{V_R}\right)t} \quad \text{[Eq. 3]}$$

Where M is the total amount of substance (nmol) in the system, $C_R(t)$ is the theoretical receiver concentration and $C_{R,0}$ is the initial receiver concentration. According to protocol, P_{app} could be calculated by first calculating an initial guess of P_{app}, obtained under sink condition. The P_{app} could then be solved with curve fitting of equation 3 to minimizing the sum of squared errors between theoretical receiver concentrations and measured receiver concentrations. The P_{app} and FA_{cum} of D-mannitol transport was analysed under non-sink conditions while under sink conditions for sucralose transport.

2.2 Effects of obesogens on tight junction protein expression

2.2.1 Caco-2 cell culture and exposure to obesogens

Caco-2 cells (P-104) were cultured and harvested as previously described and seeded on a TPP® 6-well tissue culture plate at a cell concentration of ~1 x 10^5 cells/well. Cells were cultured in DMEM-PEST, with medium change every second day. When reaching ~90 % confluence (after ~7 days) cells were washed with DPBS(-). DMEM-PEST, without phenol red, and BPA, BPAF, Imi and TBT-Cl (each diluted in DMSO) were added to the cells in duplicates with final concentration of 10 nM. The cells were exposed to the obesogens for 48 h after which the cells were harvested as previously described, but with DPBS(-) washing after resuspension. The cell count of one sample was calculated and the remaining samples were assumed to have an equal amount of cells. All samples were lysed with 100 µL radioimmunoprecipitation assay (RIPA) buffer containing the protease inhibitor Complete™-mini and EDTA (approximately 100 µL RIPA per 1 x 10^6 cells). The lysis was performed for ~60 min on ice with constant agitation on plate shaker, with vortexing and a couple of seconds of sonication every 10 min, followed by shearing of cell lysate through a 23 G syringe needle. The cell samples were spun down at 14 000 g for about 30 min at 4 °C. The supernatants were transferred to new tubes and stored at -20 °C.

2.2.2 DC protein assay

The Bradford assay could not be applied because the detergents in the RIPA buffer can interfere with the protein and dye interaction. Hence, a Bio-Rad DC™ protein assay was performed. A reagent A' solution was prepared by mixing 20 µL of Bio-Rad DC™ protein assay reagent S for each mL of alkaline copper tartrate solution (reagent A). Protein extracts from cell lysis were 2X serial diluted (up to 16X) in lysis buffer. Three µL of samples and bovine serum albumin (BSA) standards, 2X serial diluted from 20 µg/µL in water, were loaded in duplicates on Greiner transparent 96 well plates. Three µL of blanks, water for standards and lysis buffer for samples, were also loaded in duplicates on the plates. Fifteen µL of reagent A', and 120 µL of dilute folin reagent (reagent B) were added to each well. Plates were put on a plate shaker for ~15 min, after which absorbance was measured at 750 nm using a plate reader. BSA standards absorbance and protein concentrations were determined using the Magellan™ data analysis software.

2.2.3 SDS-PAGE and WB

Protein extracts were diluted to equal concentrations and mixed with 4X Laemmli sample buffer (3:1). Twenty-four µg of protein from each sample and 5 µL Precision plus protein™ WesternC™ standard were loaded onto 12 % Mini-Protean® TGX™ precast gel, set up in a Mini-Protean® tetra cell with 1X running buffer containing 3 g/L 2-Amino-2-(hydroxymethyl)-1,3-propanediol (TRIS base), 14.4 g/L glycine and 1 g/L sodium dodecyl sulfate (SDS) in purified water. SDS-polyacrylamide gel electrophoresis (PAGE) was carried out initially at 40 V for 10 min followed by 100 V for ~90 min. Immun-blot® polyvinylidene fluoride (PVDF) membranes (0.2 µM) were precut and activated in methanol (99 %) for ~1 min. Membranes and gels were rinsed with water and equilibrated in 1X transfer buffer containing 3.03 g TRIS base and 14.4 g glycine in 0.78 M methanol, for 15 min. Precut thick blot filter papers (9.5 x 15.2 cm) were soaked in 1X transfer buffer and sandwiches were assembled. Sandwiches were then set up in a Criterion™ blotter with 1X transfer buffer. The transfer was run for ~12 h at 10 V in cold room (4 °C) with constant stirring. Transfer membranes and gels were rinsed in purified water. Membranes were air dried and stored between two filter papers and sealed from air in plastic film. Gels were stained with ultrapure Coomassie brilliant blue G ultrapure to confirm separation. Membranes were stained with Ponceau S solution to confirm transfer.

2.2.4 Dot blots to optimize background noise

Dot blots were performed to optimize protocol for the WB method. This was done by study if there was an eventual correlation between type of PVDF membrane and effect on background noise. Dot blots on Amersham™ Hybond™ P 0.45µm PVDF membranes and Immun-blot® PVDF membranes were compared. The membranes were activated in methanol, rinsed with water and blotted with ~30 µg protein, from Caco-2 cell lysate, and left to air dry on filter paper. The membranes were then blocked in 3 % BSA in TRIS base buffered saline (pH ~7.6) with 0.1 % Tween 20 (TBST). After blocking for ~1.5 h, the membranes were washed 3 x 5 min in TBST. The primary polyclonal rabbit IgG Abs (Abs) ZO-1, JAM-A, and claudin-2 were diluted 1:2000, 1:1000 and 1:500 respectively in TBST (3% (w/v) BSA and ~0.02% (w/v) sodium azide). Membranes were incubated on shaker in primary Ab solutions for ~1 h. Membranes were washed 3 x 5 min followed by incubation with secondary Ab: goat anti-rabbit IgG horseradish peroxidase (HRP) conjugate diluted 1:20 000 in TBST. Membranes were washed 3 x 5 min, followed by chemiluminescence signal development with Clarity™ western enhanced chemiluminescence (ECL) blotting substrate. Images were captured using Chemidoc™ XRS+ system with Image lab™ software. Further, a comparison of background noise from different blocking agents was studied. Immun-blot® PVDF membranes were blotted as described above but blocked with blotting grade blocker non-fat dry milk (hereafter dry milk) in TBST (~0.02% (w/v) sodium azide) with or without 3 % BSA.

2.2.5 Ab incubation and chemiluminescence imaging

An Ab cocktail was made on primary polyclonal rabbit IgG Abs: ZO-1, JAM-A, and claudin-2 diluted 1:500, 1:500 and 1:200 respectively in TBST (3% (w/v) BSA and ~0.02% (w/v) sodium azide). Previously stored PVDF membranes were activated in methanol (99 % analytic) and rinsed with water. Membranes were blocked in dry milk for ~1.5 h, followed by overnight incubation at 4 °C in Ab cocktail mixture sealed in plastic film and placed on shaker. Membranes were washed 5 x 5 min in TBST, succeeded by an extra blocking step for ~45 min, after which washing was repeated. The secondary Ab goat anti-rabbit IgG HRP conjugate (1:100 000) and the precision protein™ streptactin-HRP conjugate (1:10 000) were diluted in TBST. Membranes were incubated for ~1 h on shaker in the secondary Ab solution followed by washing 5 x 5 min in TBST. Chemiluminescence signals were developed with Clarity™ western ECL blotting substrate kit. Images were captured using ChemiDoc™ XRS+ System with Image Lab™ Software.

2.2.6 Stripping and reprobing of membranes

For densitometry comparison Abs were stripped from membranes, in 1X stripping buffer (15 g/L glycine, 1 g/L SDS and 1 % Tween 20 in Milli-Q® water, pH adjusted to ~2.2). The membranes were incubated at room temperature on a shaker in 1X stripping buffer for 10 min and repeated once with fresh buffer. Then the membranes were washed 2 x 10 min in PBS and 2 x 5 min in TBST. Succeeding with blocking the membranes with dry milk for ~1.5 h. Membranes were incubated overnight at 4 °C on shaker in primary Ab anti-glyceraldehyde 3-phosphate dehydrogenase (GAPDH) rabbit IgG (1:2000) diluted in TBST (3 % (w/v) BSA and 0.02 % (w/v) sodium azide), sealed in plastic film. The membranes were washed 5 x 5 min in TBST, succeeded by an extra blocking step for ~45 min, after which washing was repeated. The secondary Ab goat anti-rabbit IgG HRP Conjugate (1:100 000) and the precision protein™ streptactin-HRP Conjugate (1:10 000) were diluted in TBST. Membranes were incubated for ~1 h on shaker in the secondary Ab solution followed by washing 5 x 5 min in TBST. Chemiluminescence signals were developed with Clarity™ Western ECL blotting substrate kit. Images were captured using ChemiDoc™ XRS+ System with Image Lab™ Software.

2.3 Epigenetic effect of obesogens on tight junction protein expression

The study of epigenetic effect used the same method procedure outline as described in section 2.2 but with exceptions. Caco-2, P-104, were cultured on four 6-well plates after which monolayers were treated in duplicates with 50 nM of respective obesogen. After two days the obesogen treatment was ended for one set of the duplicates by first washing the samples with DPBS(-) and then continued culturing with regular medium. After six days both sets of the duplicates were harvested as previously described. Hence one set of duplicates had been exposed for two days and the other for six days. Cells were harvested and lysed as previously described. Protein transfer for WB was run for ~16 h at 15 V. The transfer was done with thick blot filter paper, 9.5 x 15.2 cm for BPA/BPAF and 7.5 x 10 cm for Imi/TBT-Cl treated cells.

2.4 Evaluation of ZO-1, JAM-A and claudin-2 Abs

To evaluate specificity of Abs the membrane from 10 nM Imi or TBT-Cl treatment (for 48 h) was stripped and reprobed with ZO-1 (1:200) diluted in TBST (3 % (w/v) BSA and 0.02 % (w/v) sodium azide). Chemiluminescence signal was captured and membrane was stripped and reprobed with primary Ab-cocktail of JAM-A (1:200) and claudin-2 diluted in TBST (3 % (w/v) BSA and 0.02 % (w/v) sodium azide).

2.5 Permeability test using multiple permeability markers

2.5.1 Permeability assay

The function of TJs was impaired with the use of sodium caprate (C10) to increase the permeability of the Caco-2 cell monolayer [21]. A stock solution of 0.112 M C10 (pH ~6.85) was prepared. This was done by first liquefying capric acid in water bath (35°C) followed by neutralization with NaOH (0.050 M) and HBSS(-). A three-fold serial dilution of the stock solution was made six times in HBSS(-). Permeability marker solutions were prepared by adding 0.025 M of BPA, BPAF, Imi and TBT-Cl in DMSO, sucralose and D-mannitol (0.025 M) to purified water. Equal volumes of permeability markers and HEPES buffer (1 M) were added to the series. The final concentrations were as following: 108, 36, 12, 4, 1.330, 0.444 and 0.148 mM of C10; 0.100 mM obesogens; 2 mM sugars and 25 mM HEPES buffer. A negative control solution was prepared with permeability markers in HBSS(-).

Caco-2 cells (P-103) were cultured and harvested as previously described, and seeded at a density of 60 000 cells/well on a Millicell® 24-well cell culture plate for ~25 days. Medium was removed and cell monolayers washed twice with HBSS(-) for 15 min in incubator. 400 µL of the seven different permeability marker solutions were added in triplicates to apical wells and 150 µL samples of each one were immediately collected. 800 µL of HBSS with calcium and magnesium (HBSS(+)), were added to

the basolateral side of the wells. The plate was put in incubator at 37 °C, 10% CO_2 and ~95% humidity. Every 20 min, 260-440 µL samples were collected from the basolateral side and replaced with fresh HBSS(+) for 60 min, after which 150 µL apical samples were collected. Samples and plate were stored at -20 °C.

2.5.2 HPLC and permeability marker analysis

A sucralose HPLC assay was performed twice on one of each triplicate samples collected from the permeability assay with sucralose, D-mannitol and obesogens as markers. Stored samples were thawed and vortexed. The apical samples were diluted four-fold while most of the basolateral samples were kept undiluted. The samples were spun down at 2500 RCF at 4 °C for 10 min. For each run, 120 µL of sample was injected into a Gilson HPLC apparatus connected to an evaporative light scatter detector, where sample components were detected during 20 min. Data was collected with Gilson UniPoint 2.0 software and transferred to SigmaPlot (statistical plotting software). Each sample duplicate set of data were simultaneously plotted and peaks were identified at around 9 min. Peaks were manually aligned if needed. The area of each peak was calculated by summarizing all point values and subtracting the baseline area, which was calculated by multiplying number of data points to the average of the first and last three mean values in the series. Each calculated peak area was compared and if not significantly different, the mean area of the peaks was calculated. With the slope of a sucralose standard curve the concentration could be determined by

$$Sample\ concentration = mV \times K + M \qquad \text{[Eq. 4]}$$

Where mV is the calculated mean peak, K is the slope of the standard curve and M is the intercept. Thus the sucralose concentration of every sample could be calculated. Note that due to lack of time an already made sucralose standard curve was used, and this creates issues with background. P_{app} was determined under sink conditions as described in section 2.1.6.

3. Results

3.1 Transport of D-mannitol across obesogen exposed Caco-2 cell monolayers

3.1.1 D-mannitol concentrations

The standard curve of the 3X dilution series of D-mannitol (Fig. 3) was used for further determination of D-mannitol concentrations.

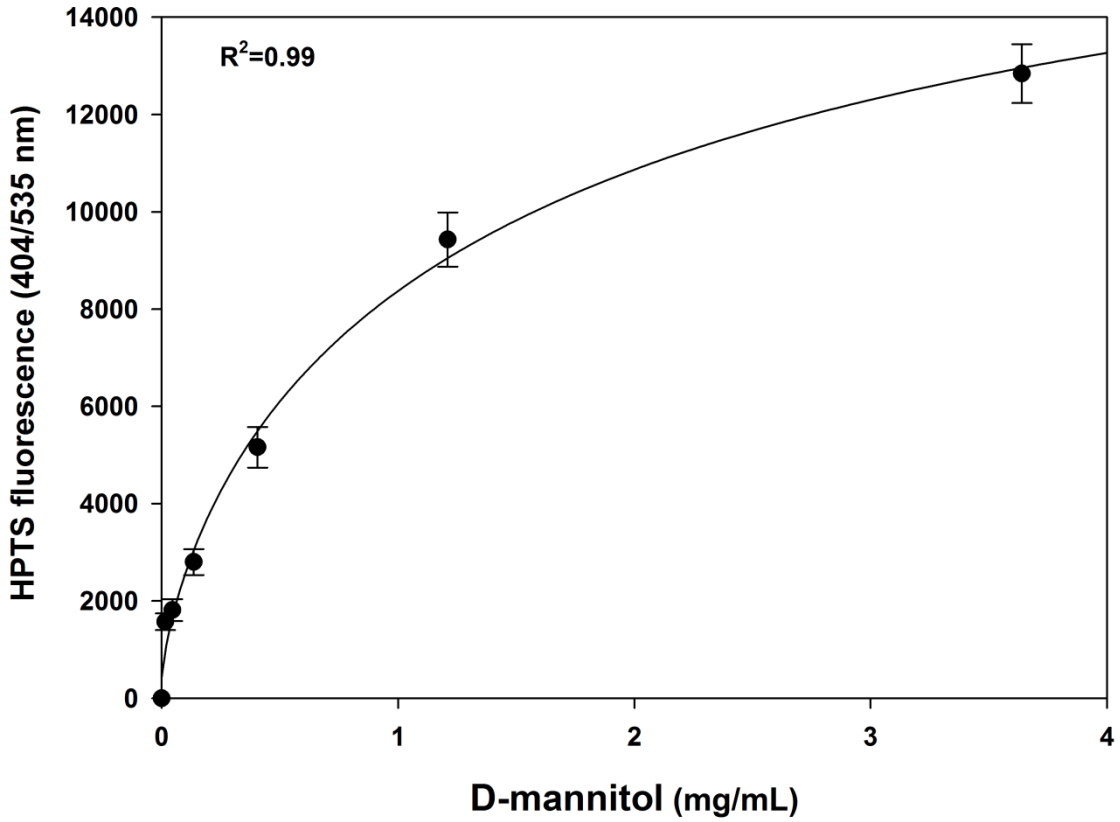

Figure 3. D-mannitol standard curve obtained from the 4,4'oBBV assay. The curve has the following equation y = 418.1314 + (19887.0312 - 418.1314) / (1 + (x / 1.6418)$^{-0.7451}$), where y and x represent fluorescence and concentration respectively.

3.1.2 Analysis of D-mannitol transport

The D-mannitol mass, derived from the concentration determination, for each respective sampling point was compared (Fig. 4). The expected result was that the mass of D-mannitol in the apical side would decrease from 0 to 60 min. This could not be observed for most of the cases, the majority of the samples showed on the contrary an increase of D-mannitol mass in the apical side from 0 to 60 min. This was especially true for Imi and TBT-Cl samples, which showed much higher mass of D-mannitol in apical side at 30 or 60 min compared to the mass at 0 min. Further, the initial mass (apical at 0 min) for BPA, BPAF and Imi samples were relatively close to the theoretical mass (~0.15 mg). However, the control for Imi and TBT-Cl together with all samples from TBT-Cl showed much lower mass than the theoretical. Another expected result was that the mass in the basolateral side at 30 and 60 min would be lower or equal (complete permeation) to that of apical at 0 min. This could be observed for all samples at the 30 min mark, but not for all of the samples at the 60 min mark. In addition, the observed mass at the 60 min mark was not the total mass since the removed sample (for concentration measurements) at the 30 min mark was not included.

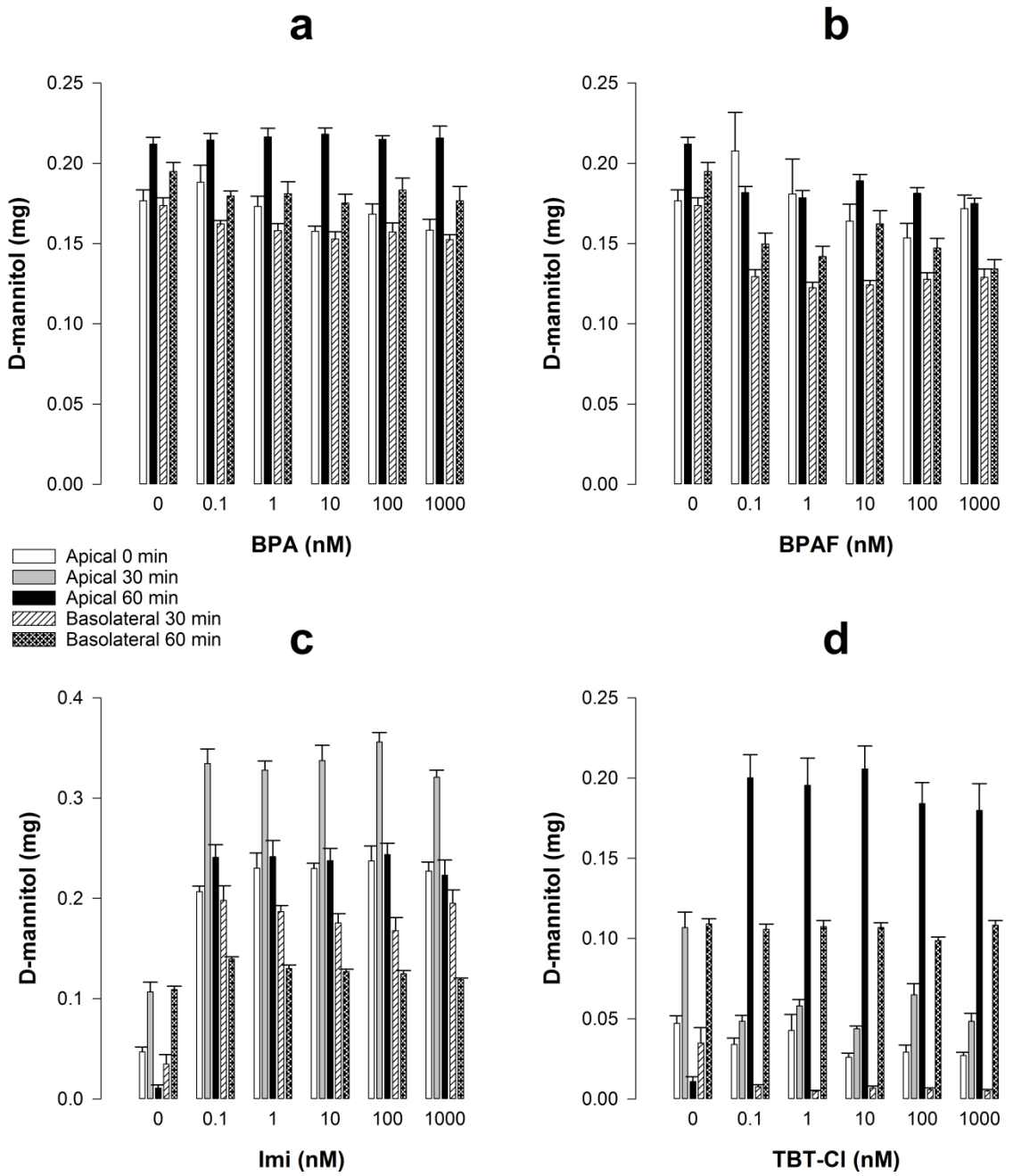

Figure 4. D-mannitol apical to basolateral permeation across Caco-2 cell monolayers exposed to 0.1, 1, 10, 100 or 1000 nM of respective obesogen for 48 h. 0 nM is the negative control which is the same for BPA and BPAF and the same for Imi and TBT-Cl. **(a)** Show cells treated with BPA, **(b)** BPAF, **(c)** Imi and **(d)** TBT-Cl. The bars indicate the average amount of D-mannitol (mg) from eight separate measurements per two wells (identically exposed monolayers). Error bars are ± SEM. White bars represent apical at 0 min. Grey bars represent apical at 30 min (only sampled for Imi and TBT-Cl). Black bars represent apical at 60 min. White bars with black helical pattern represent basolateral at 30 min. White bars with black cross pattern represent basolateral at 60 min.

The total D-mannitol mass in basolateral side at 60 min was compared to the apical side at 0 min (Fig. 5). This showed that the total mass of D-mannitol at the 60 min mark was higher than the initial mass for almost all samples. This was not theoretically possible as no additional D-mannitol was added during the experiment. Consequently, only the initial mass in apical at 0 min and in basolateral side at 30 min could be used to evaluate permeation of D-mannitol. All data can be found in Appendix A.

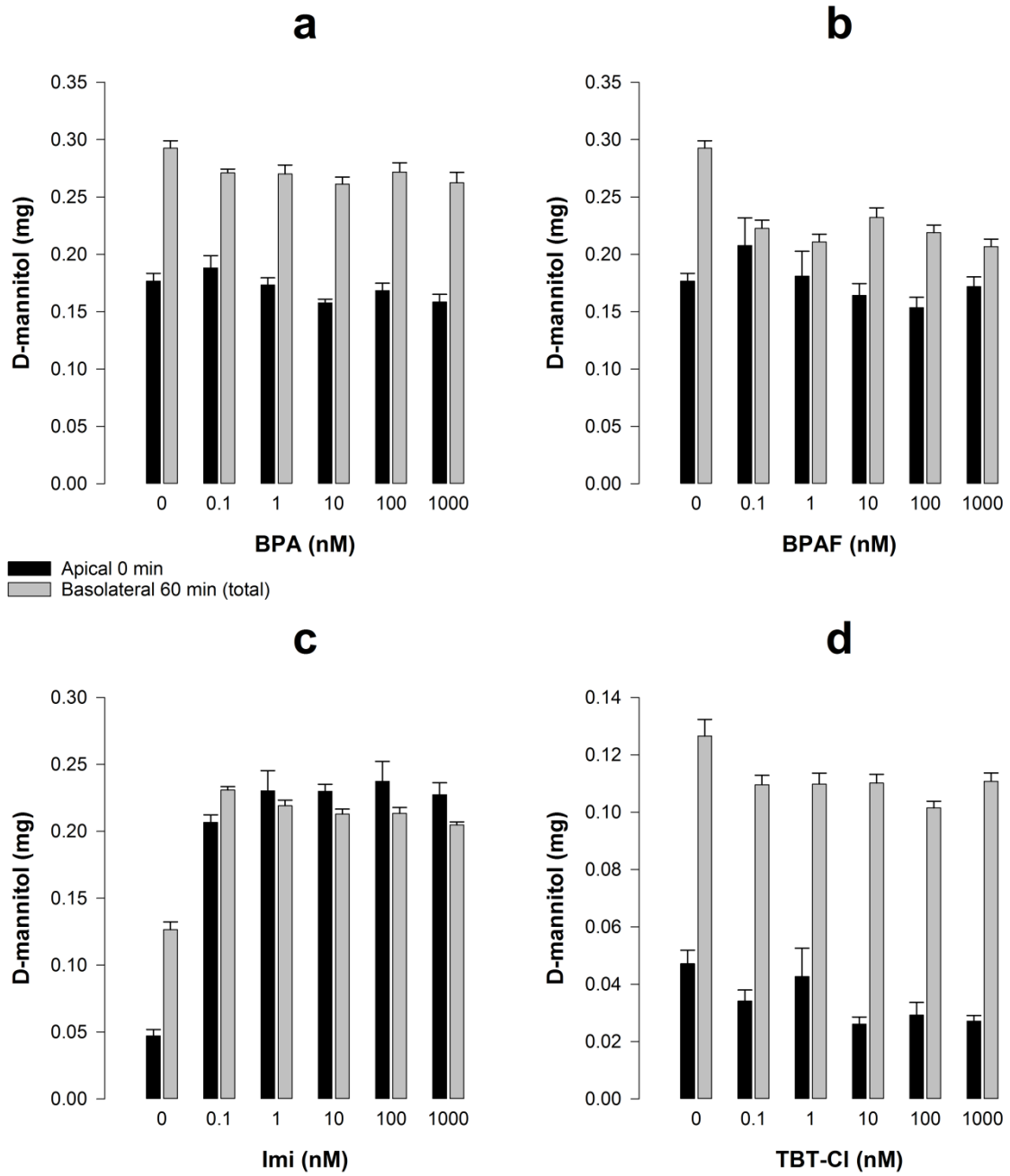

Figure 5. Total amount of D-mannitol permeation across Caco-2 cell monolayers, exposed to 0.1, 1, 10, 100 or 1000 nM of respective obesogen for 48 h. 0 nM is the negative control which is the same for BPA and BPAF and the same for Imi and TBT-Cl. **(a)** Show cells treated with BPA, **(b)** BPAF, **(c)** Imi and **(d)** TBT-Cl. Black bars represent average amount of D-mannitol (mg) at apical side at 0 min. Grey bars illustrate the calculated total amount of D-mannitol (addition of measured amount in basolateral side at 60 and 30 min). Error bars represent ± SEM (propagated for grey bars).

The approximate percentage permeation of D-mannitol was used to obtain an indicative whether the obesogens affect permeability of D-mannitol across Caco-2 monolayers (Fig. 6). The BPA samples did not show a notably difference compared to the control. The BPAF samples did show a notably difference, especially for the lower concentrations of BPAF (0.1 and 1 nM). This could imply that low concentrations ($\leq$ 1 nM) of BPAF reduce permeability of D-mannitol across Caco-2 cell monolayers. On the contrary, the low concentrations of Imi samples implied an increased permeability compared to the control. The TBT-Cl samples showed a significant reduce in permeability for all concentrations. All data can be found in Appendix B.

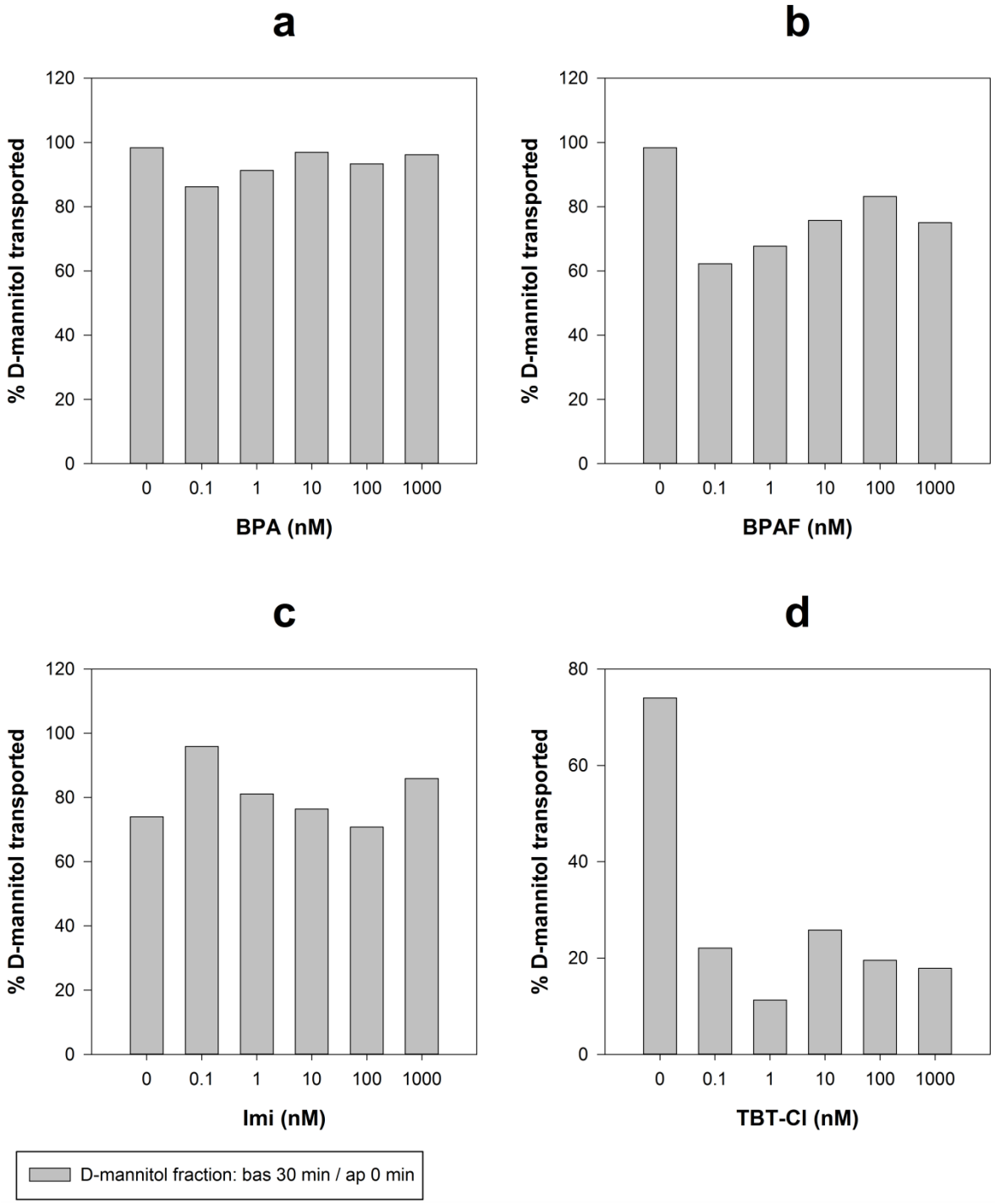

Figure 6. Percentage of D-mannitol permeation, from apical at 0 min to basolateral 30 min, across Caco-2 cell monolayers, exposed to 0.1, 1, 10, 100 or 1000 nM of respective obesogen for 48 h. 0 nM is the negative control which is the same for BPA and BPAF and the same for Imi and TBT-Cl. **(a)** Show cells treated with BPA, **(b)** BPAF, **(c)** Imi and **(d)** TBT-Cl. The grey bars illustrate the percentage amount of D-mannitol permeated from the apical side at 0 min to the basolateral side at 30 min.

3.1.3 The apparent permeability coefficient for D-mannitol transport

The P_{app} calculations of D-mannitol permeation was not applicable since the function of the nonlinear curve fitting tool in Excel was limited by producing unequal results in successive runs (data not shown).

3.2 Dot blots

No significant difference in background noise based on type of PVDF membrane or on primary Abs was detected (Fig. 7a-c). Type of diluent used for secondary Abs does however have an impact on background noise (Fig. 7d). The blots show that secondary Abs are promoting signal without any primary Abs to a higher degree when using a 3 % BSA in the TBST diluent compared to only TBST. This implies that BSA is aiding in binding of secondary Abs, giving rise to false signals. The result also indicates that the concentration of secondary Abs is too high since they produce a signal, even when diluted in only TBST. Dot blots with less concentrated secondary Abs established appropriate dilution ratios (1:100 000) (figures not shown).

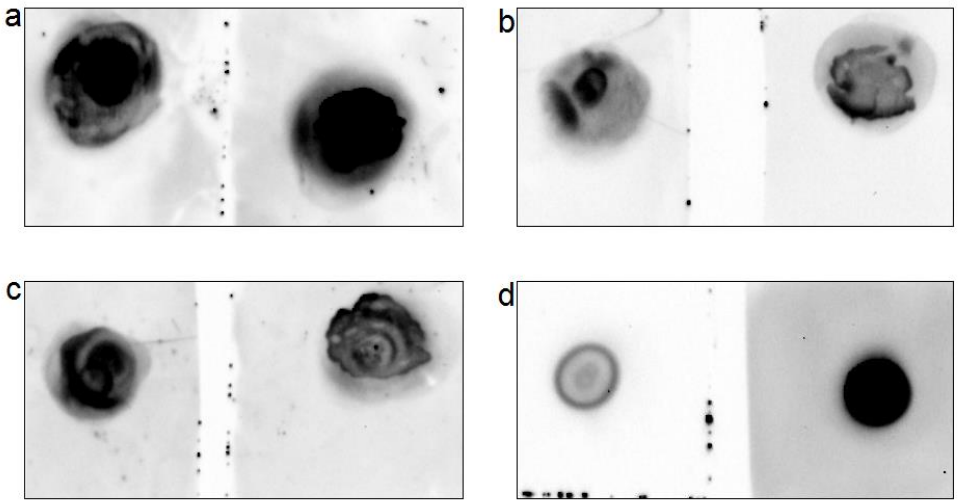

Figure 7. Effect of PVDF membrane type and secondary Ab diluent type on background noise. Secondary Ab: Goat anti-rabbit IgG HRP Conjugate used on each dot blot. **(a - c)** Left dot blots are on PVDF Transfer Membrane (0.45 µM) and right on Immun-Blot® PVDF membranes, all with ~30 µg Caco-2 protein extracts and with primary Abs: **(a)** ZO-1, **(b)** claudin-2 and **(c)** JAM-A. **(d)** Both dot blots are on Immun-Blot® PVDF membranes with ~30 µg Caco-2 protein extracts and without primary Abs, where the left use secondary Ab diluted in TBST and right in TBST (3 % BSA).

3.3 Effect of obesogens on tight junction protein expression

3.3.1 Protein concentrations from cells exposed to obesogens for 48 h

The protein concentrations of lysate from cells exposed to 10 nM of individual obesogens for 48 h were analysed (Table 1). The difference between the concentrations was considerably high since a range of 2.4-9.9 µg/µL implies approximately four times more protein in the highest concentrated sample.

Table 1. Protein concentrations of Caco-2 cells (P-104) treated with BPA, BPAF, Imi or TBT-Cl for 48 h. The absorbance was measured at 750 nm. Each value is the mean protein concentration (µg/µL) ± SEM of a serial dilution. Every sample was measured in duplicates.

Control (BPA/BPAF)	BPA	BPAF	Control (Imi/TBT-Cl)	Imi	TBT-Cl
9 ± 0.3	6.1 ± 0.5	6.7 ± 0.4	3.1 ± 0.5	9.9 ± 0.8	6.5 ± 1.6
8.8 ± 0.2	6.3 ± 0.5	6 ± 0.4	5.1 ± 0.7	4.7 ± 0.8	2.4 ± 0.5

3.3.2 WB chemiluminescence images (48 h)

The presence of TJ proteins were determined by studying WB images of membranes incubated with either a primary Abs cocktail consisting of ZO-1, JAM-A and claudin-2 (Fig. 8a and c) or GAPDH (Fig. 8b and d). Protein bands for ZO-1 (220 kD), JAM-A (36 kD) and claudin-2 (25 kD) could not be identified for neither BPA/BPAF (Fig. 8a) nor Imi/TBT-Cl (Fig. 8b). Weak signals at 37 kD is most

likely GAPDH (37 kD) and not JAM-A as these bands are very similar in both size and shape. Further, the multiple bands detected between 150 – 50 kD are likely to be the result of poor specificity of either of the primary Abs.

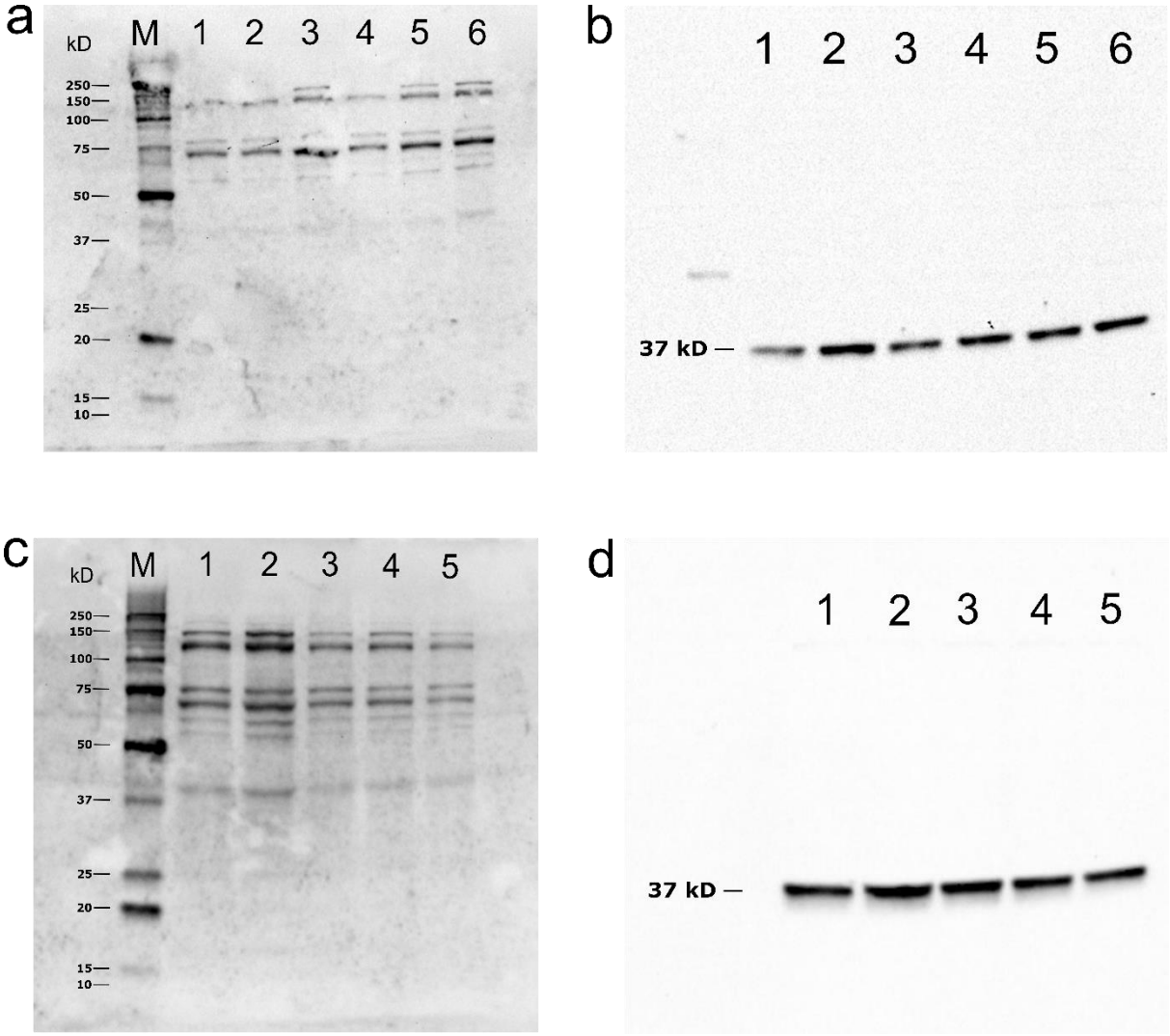

Figure 8. WB chemiluminescence images from 10 nM of BPA, BPAF, Imi or TBT-Cl treatment for 48 h. (**a**) BPA or BPAF treated cells, where lanes 1 and 2 are control replicates, lanes 3 and 4 are BPAF replicates and lanes 5 and 6 are BPA replicates, all with primary Ab cocktail: JAM-A, ZO-1 and claudin-2. (**b**) Same sample order as (**a**) but with GAPDH primary Ab. (**c**) Imi or TBT-Cl treated cells, where lanes 1 and 2 are control replicates, lanes 3 and 4 are Imi replicates and lanes 5 and 6 are TBT-Cl replicates, all with primary Ab cocktail: JAM-A, ZO-1 and claudin-2. (**d**) Same sample order as (**c**) but with GAPDH primary Ab. Lane M received MW standards.

3.3.3 Staining of gels and membranes (48 h)

Coomassie staining of SDS-PAGE gels for obesogen treated cells (Fig. 9a and c) illustrates that the WB transfers are somewhat incomplete as both gels have residual proteins between 250 – 100 kD. This indicates that the transfer protocol needs adjustment. Further, the Ponceau stained WB membranes (Fig. 9b and d) showed that protein had transferred for all samples.

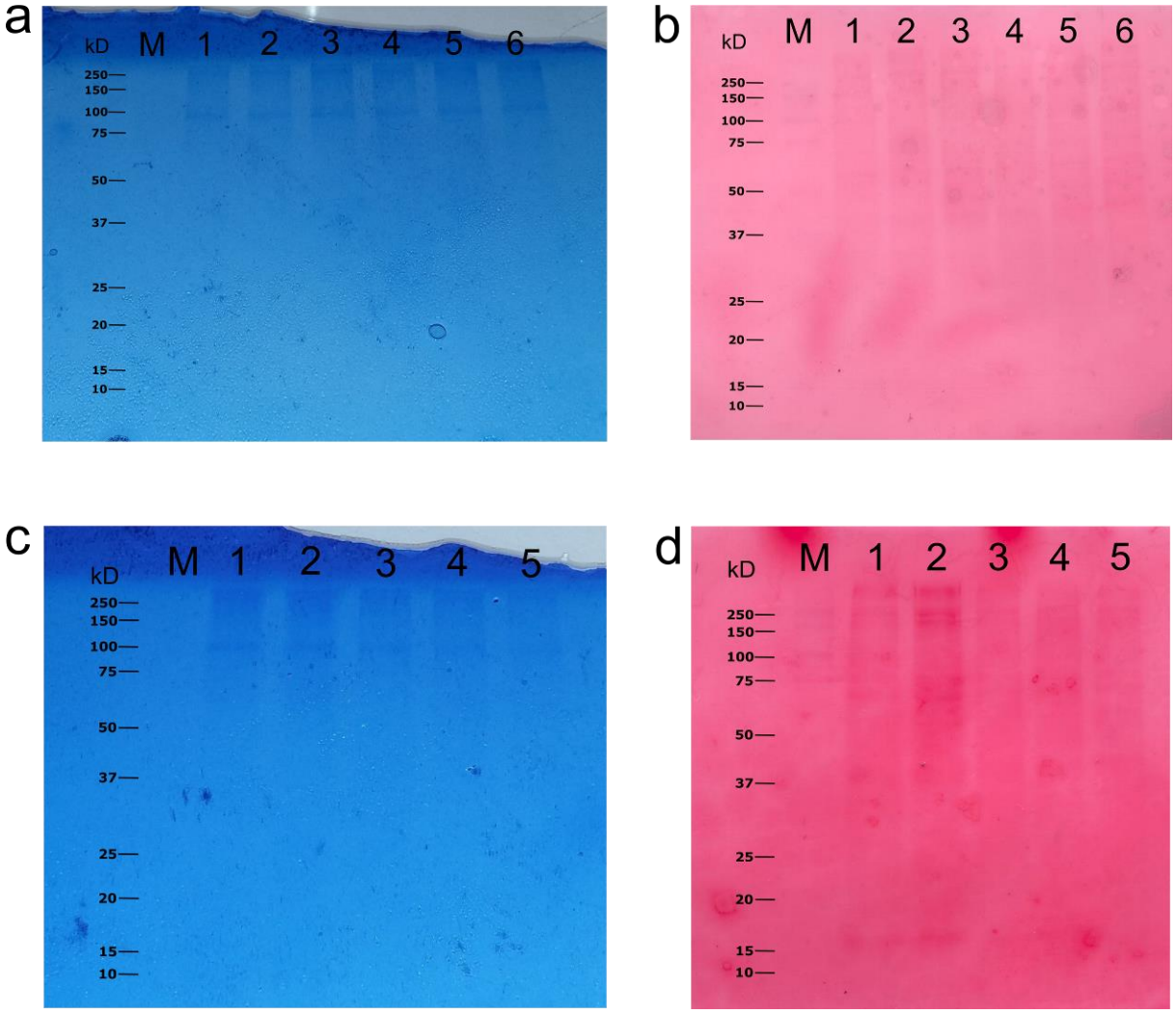

Figure 9. SDS-PAGE gel and WB membrane staining from 48 h, 10 nM obesogen treated cells. (a) Brilliant Blue G ultrapure stained gel, 1-2: control, 3-4: BPAF and 5-6: BPA. (b) Ponceau S stained membrane, with same sample order as (a). (c) Brilliant Blue G ultrapure stained gel, 1: control, 2-3: TBT-Cl and 4-5: Imi. (d) Ponceau S stained membrane, with same sample order as (c). Lane M is MW marker.

3.4 Epigenetic effect of obesogens on TJ protein expression

3.4.1 Protein concentrations from cells exposed to obesogens for 2 or 6 days

The protein concentrations of lysate from cells exposed to the individual obesogens (50 nM) for 2 or 6 days were compared and analysed (Table 2). The difference range of 1.4-4.1 µg/µL between sample concentrations implies approximately three times more protein in the highest concentrated sample.

Table 2. Protein concentrations of cells treated with 50 nM BPA, BPAF, Imi or TBT-Cl for 2 days or 6 days. Absorbance measured at 750 nm. Each value is the mean protein concentration (µg/µL) ± SEM of a serial dilution. C refers to control treatment. The experiments were performed in duplicates.

Days exposed	Protein concentration (µg/µL)			
	BPA	BPAF	Imi	TBT-Cl
2 days	3.9 ± 0.3	3.1 ± 0.5	1.9 ± 0.4	2.1 ± 0.4
2 days	4.1 ± 0.6	2.5 ± 0.6	1.9 ± 0.4	1.9 ± 0.4
6 days	3.5 ± 0.8	2.9 ± 0.4	1.4 ± 0.1	1.6 ± 0.1
6 days	3.5 ± 0.4	1.9 ± 0.4	1.5 ± 0	2.2 ± 0.5
2 days (C)	3 ± 0.4	2.5 ± 0.2	2.2 ± 0.4	2.7 ± 0
6 days (C)	3.8 ± 0.5	2.1 ± 0.3	1.9 ± 0.4	1.8 ± 0.4

3.4.2 WB chemiluminescence images (2 or 6 days)

The presence of TJ proteins were determined by studying WB images of membranes incubated with either a primary Abs cocktail consisting of ZO-1, JAM-A and claudin-2 or GAPDH (Fig. 10). No signal from ZO-1, JAM-A or claudin-2 could be detected for BPA (Fig. 10a) or BPAF (Fig. 10c). A signal from GAPDH could however be detected for both BPA (Fig. 10b) and BPAF (Fig. 10d). There are distinct bands at around 75 kD, which is not the target size of either Abs, for both BPA and BPAF (Fig. 10a and c). This indicates either poor specificity of either of the Abs or proteolysis of ZO-1 proteins, as there is also no signal at around 220 kD. The signals from the other Abs, JAM-A and claudin-2, are ambiguous as the lanes are smudged, but still there are bands at 36 kD and 25 kD for both BPA and BPAF. The stripping and reprobing with GAPDH were successful as distinct band are detected at 37 kD, even though the stripping of the previous Abs were not entirely complete.

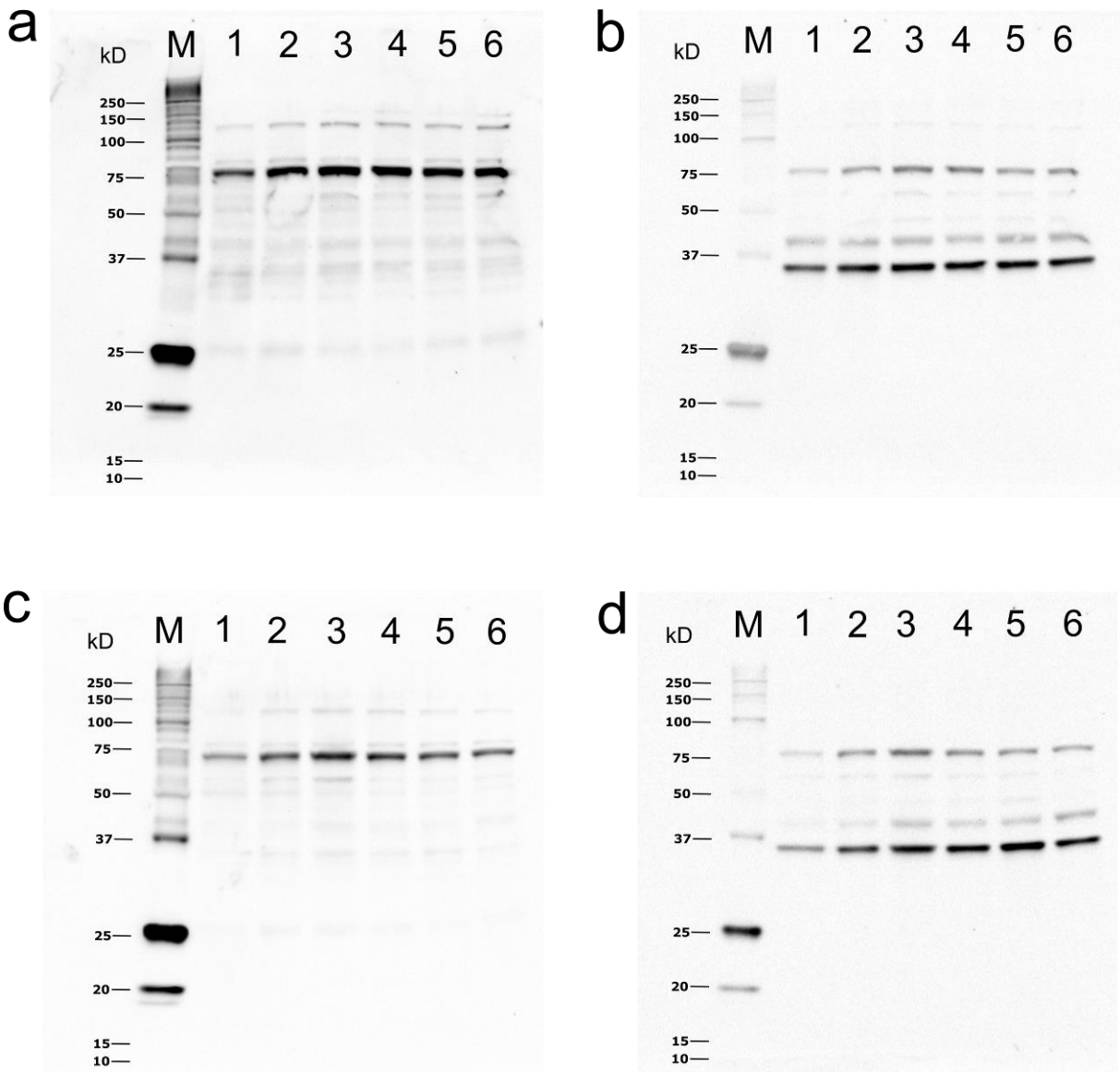

Figure 10. WB chemiluminescence images from 50 nM of BPA or BPAF treatment for 2 or 6 days. **(a)** BPA treatment, where lanes 1 and 2 are control replicates, lanes 3 and 4 are 6 days replicates and lanes 5 and 6 are 2 days replicates, all with primary Ab cocktail: JAM-A, ZO-1 and claudin-2. **(b)** Same sample order as **(a)** but with GAPDH primary Ab. **(c)** BPAF treatment, where lanes 1 and 2 are control replicates, lanes 3 and 4 are 6 days replicates and lanes 5 and 6 are 2 days replicates, all with primary Ab cocktail: JAM-A, ZO-1 and claudin-2. **(d)** Same sample order as **(c)** but with GAPDH primary Ab. Lane M received MW standards.

Similar results as previously described, were obtained for the chemiluminescence of membranes from Imi and TBT-Cl treated samples (Fig. 11). ZO-1 signal could not be detected for either membrane, but detectable signals were found JAM-A and claudin-2 at 36 kD and 25 kD (Fig. 11a and c). GAPDH gave successful signal for both Imi and TBT-Cl membranes (Fig. 11b and d). Further it is evident that the protein concentration of one of the TBT-Cl samples (lane 4) is low, indicating issues with either DC protein assay or pipetting errors.

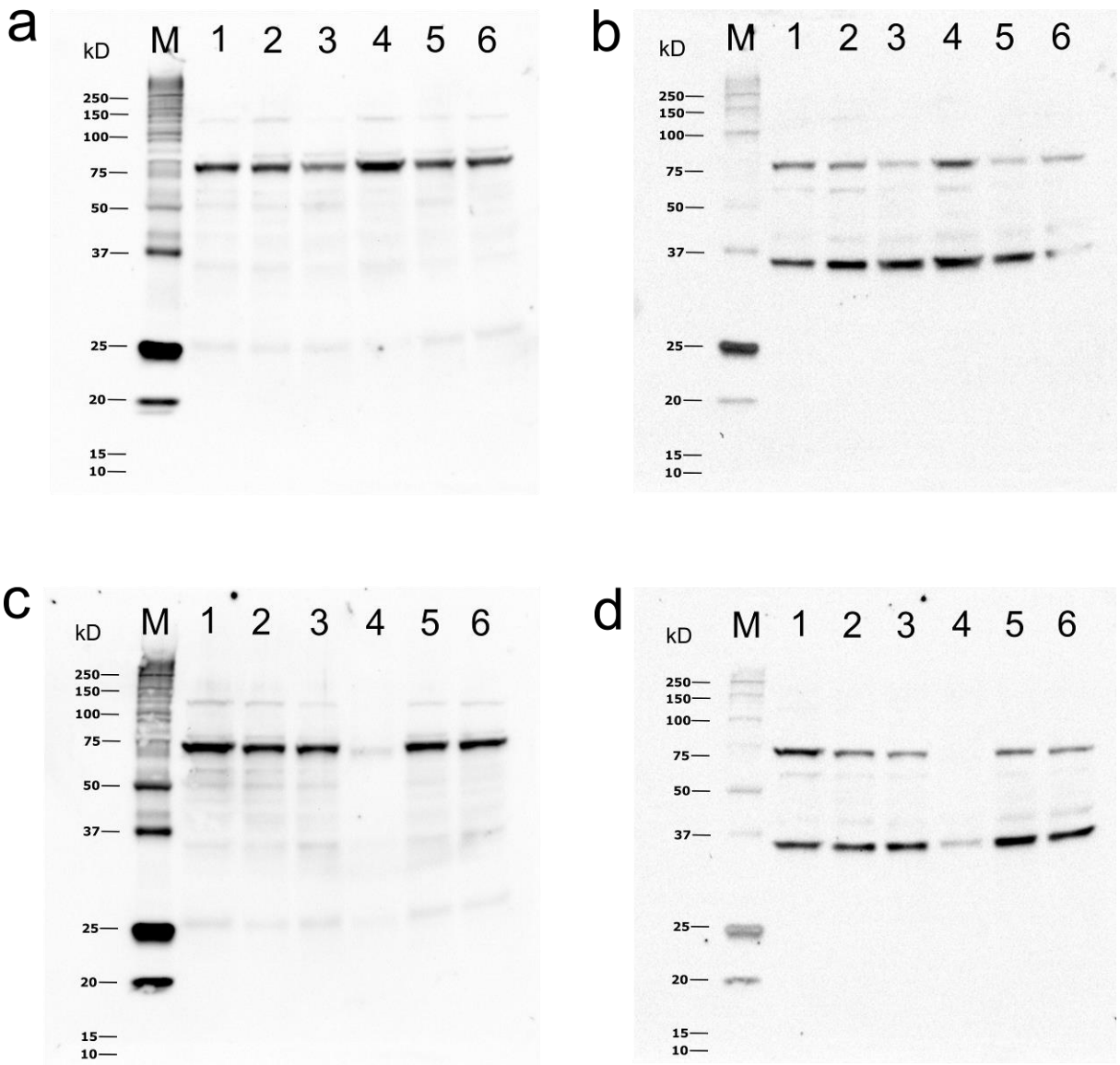

Figure 11. WB chemiluminescence images from 50 nM of Imi or TBT-Cl treatment for 2 or 6 days. **(a)** Imi treatment, where lanes 1 and 2 are control replicates, lanes 3 and 4 are 6 days replicates and lanes 5 and 6 are 2 days replicates, all with primary Ab cocktail: JAM-A, ZO-1 and claudin-2. **(b)** Same sample order as **(a)** but with GAPDH primary Ab. **(c)** TBT-Cl treatment, where lanes 1 and 2 are control replicates, lanes 3 and 4 are 6 days replicates and lanes 5 and 6 are 2 days replicates, all with primary Ab cocktail: JAM-A, ZO-1 and claudin-2. **(d)** Same sample order as **(c)** but with GAPDH primary Ab. Lane M received MW standards.

3.4.3 Staining of gels and membranes (2 or 6 days)

Gel and membrane staining from BPA (Fig. 12a and b) or BPAF (Fig. 12c and d) treated cells indicate that the transfers are still incomplete even with increased running time and voltage, compared to previous transfers (Fig. 9). Although proteins are seemingly more abundant as more distinct bands are detected on both BPA and BPAF membranes. The staining of gels and membranes from Imi (Fig. 13a and b) or TBT-Cl (Fig. 13c and d) treated cells show similar results as BPA or BPAF transfer but with unsuccessful transfer of proteins at 15 and 10 kD.

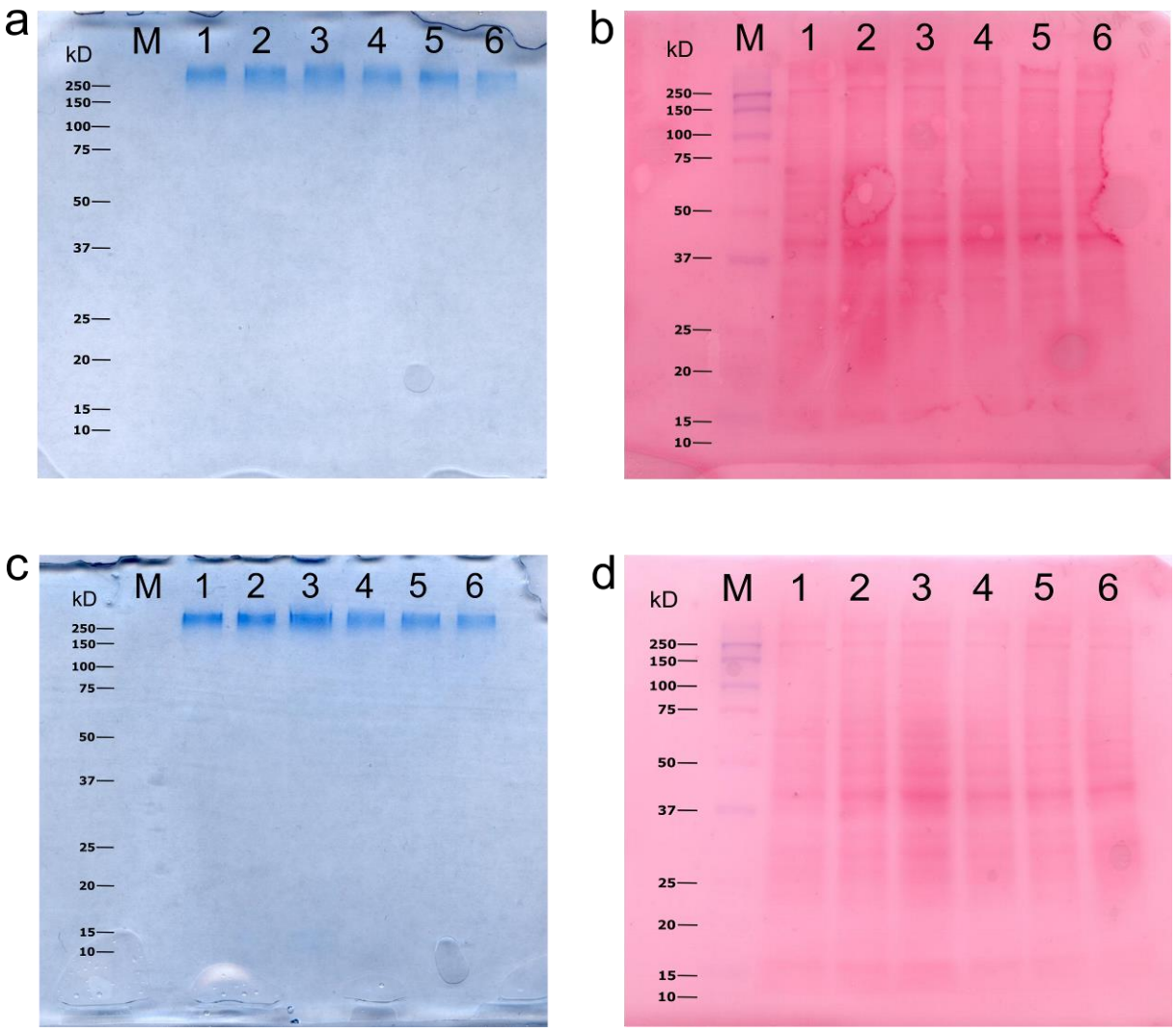

Figure 12. Stained gels and membranes for 50 nM BPA or BPAF treated cells for 2 or 6 days. **(a)** Stained gel from BPA treatment where lanes 1 and 2 are control replicates, lanes 3 and 4 are 6 days replicates and lanes 5 and 6 are 2 days replicates. **(b)** Stained membrane with sample order as **(a)**. **(c)** Stained gel from BPAF treatment where lanes 1 and 2 are control replicates, lanes 3 and 4 are 6 days replicates, and lanes 5 and 6 are 2 days replicates. **(d)** Stained membrane with sample order as **(c)**. Lane M received MW standards.

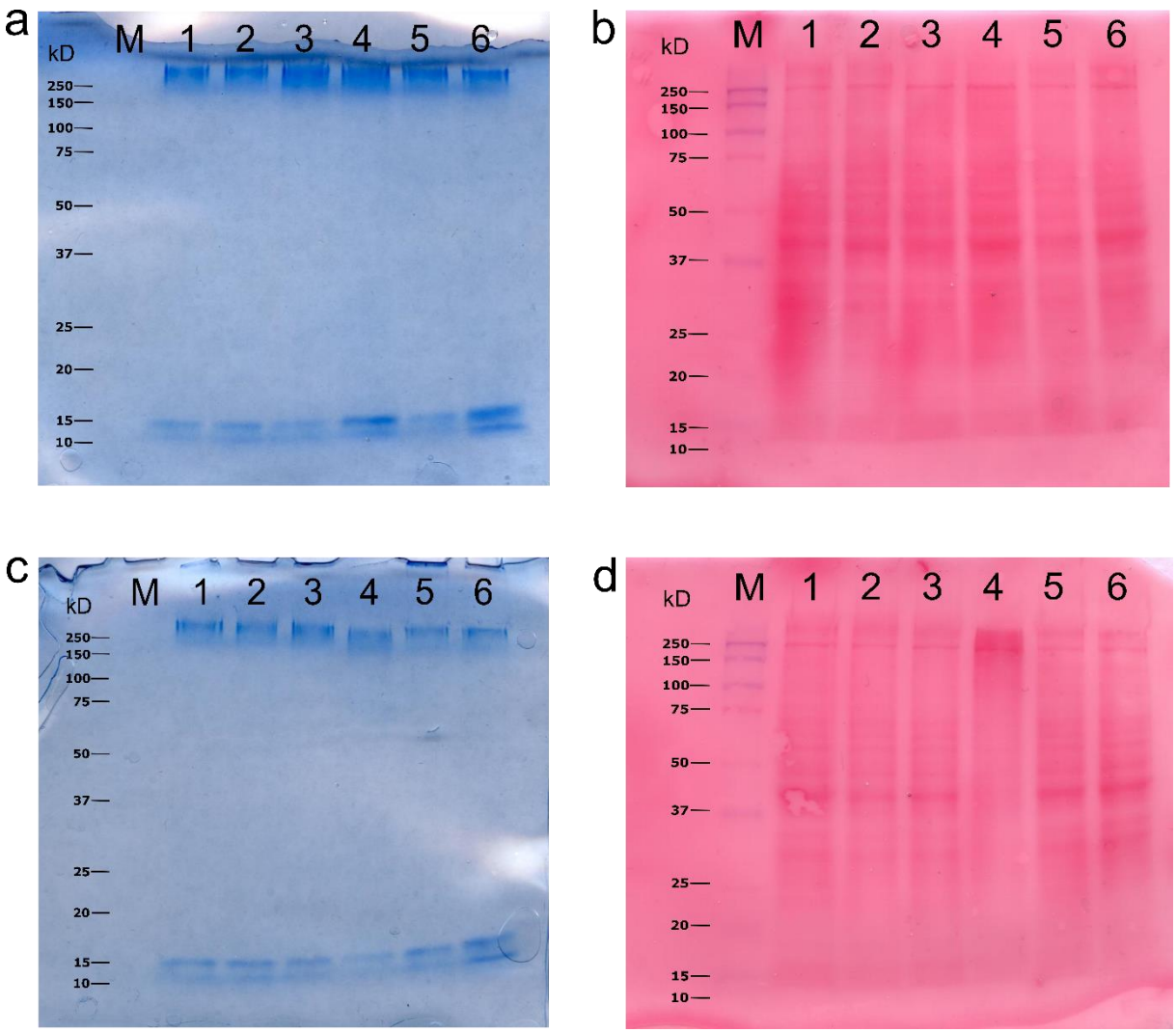

Figure 13. Stained gels and membranes for 50 nM Imi or TBT-Cl treated cells for 2 or 6 days. **(a)** Stained gel from Imi treatment where lanes 1 and 2 are control replicates, lanes 3 and 4 are 6 days replicates and lanes 5 and 6 are 2 days replicates. **(b)** Stained membrane with sample order as **(a)**. **(c)** Stained gel from TBT-Cl treatment where lanes 1 and 2 are control replicates, lanes 3 and 4 are 6 days replicates and lanes 5 and 6 are 2 days replicates. **(d)** Stained membrane with sample order as **(c)**. Lane M received MW standards.

3.5 Evaluation of primary Abs

Membranes from Imi or TBT-Cl treated cells for 48 h were incubated and reprobed with ZO-1 primary Ab (Fig. 14), and further reprobing and incubation with JAM-A and claudin-2 primary Abs (Fig. 14b). The ZO-1 incubation resulted in signals, especially at 75 kD, and residue signals of GAPDH are still present. Neither of JAM-A nor claudin-2 gave rise to signals, which further prove that the ZO-1 Ab is either nonspecific or the proteins are proteolysed.

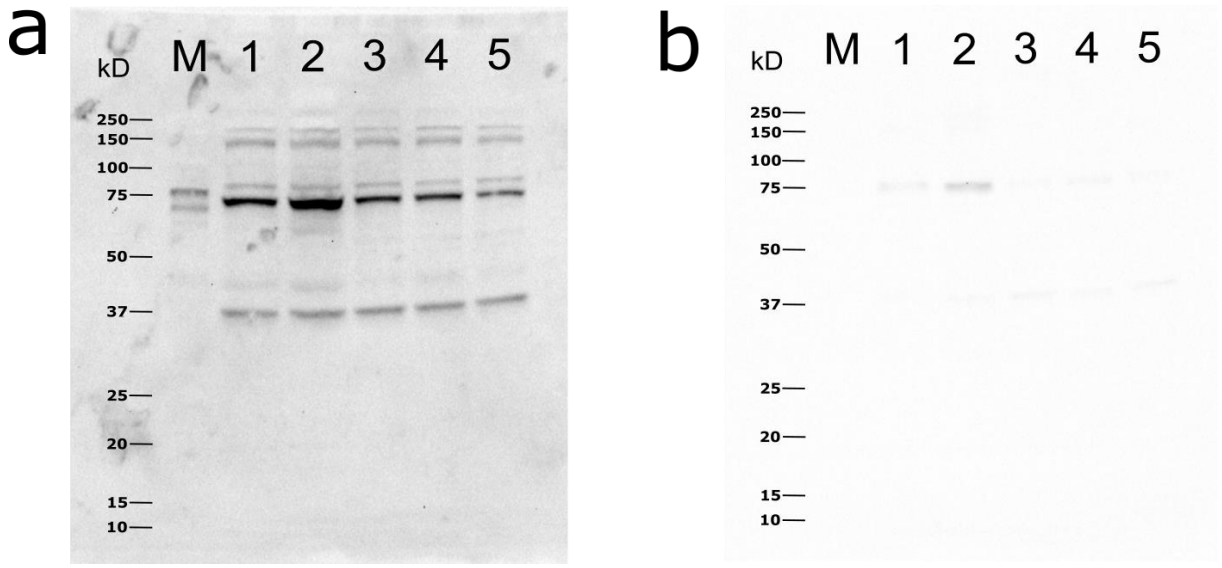

Figure 14. WB chemiluminescence images of reprobed membrane from 10 nM of Imi or TBT-Cl treatment for 48 h. **(a)** Reprobing with ZO-1 where lanes 1 and 2 are control replicates, lanes 3 and 4 are Imi replicates and lanes 5 and 6 are TBT-Cl replicates. **(b)** Reprobing with JAM-A and claudin-2 Ab cocktail with same sample order as **(a)**. Lane M received MW standards.

3.6 Transport of sucralose across C10 exposed monolayers

3.6.1 Sucralose concentrations

The HPLC measured sucralose concentrations from cells exposed to C10 were evaluated and compared to the theoretical concentration (2 mM) (Table 3). The HPLC measured amount of sucralose is reasonable, considering that 2 mM was added at apical side at the start of the permeability test, which is roughly the average of each sample. For wells treated with 12 mM C10 and above there is an indicative trend at the apical side after 60 min, where the concentration of sucralose is decreasing with increasing concentration C10. Furthermore, the basolateral concentrations of sucralose from these wells are all higher than the other wells, except for the control well (C10, 0 mM).

Table 3. HPLC measured sucralose concentrations (mM). Ap represents apical side. Bas represents basolateral side.

C10 (mM)	Sucralose (mM)				
	Ap 0 min	Ap 60 min	Bas 20 min	Bas 40 min	Bas 60 min
0	2.20	2.21	0.0132	0.0135	0.0168
0.148	2.17	2.14	0.00663	0.00668	0.00872
0.444	2.17	2.27	0.00675	0.00694	0.00720
1.33	2.01	2.20	0.00663	0.00672	0.00685
4	2.00	2.29	0.00656	0.00668	0.00701
12	1.89	1.74	0.0105	0.0460	0.0413
36	2.05	1.63	0.0102	0.0216	0.0607
108	2.09	1.43	0.0170	0.0394	0.0547

3.6.2 FA_{cum} and P_{app} of sucralose

The transport of sucralose across C10 exposed Caco-2 cells was used to evaluate if there is a correlation between the level of C10 exposure and the permeation of sucralose (Fig. 15). The FA_{cum} showed that sucralose, for wells treated with higher concentrations of C10 (12, 36 and 108 mM), were transported through monolayers approximately four times the length to that of wells exposed to lower C10

concentrations (4, 1.33, 0.444, 0.148 and 0 mM) (Fig. 15a). Similarly, the P_{app} showed that the transfer rate of sucralose was approximately six times as fast for wells exposed to higher concentrations of C10 compared to lower concentrations (Fig. 15b). All data can be found in Appendix C.

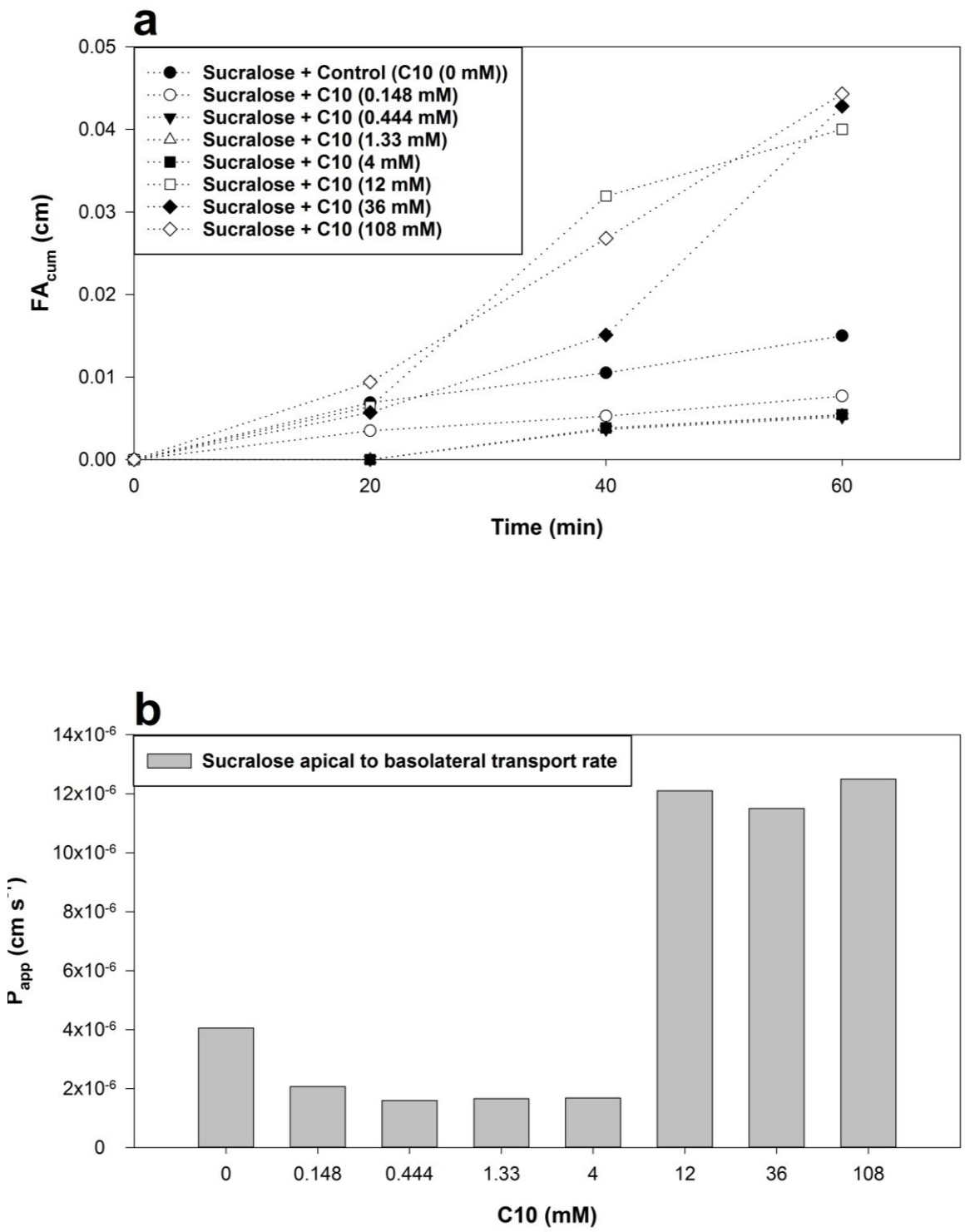

Figure 15. Effect of increasing C10 concentration on Caco-2 cell permeability. **(a)** Effect of increasing concentration C10 on sucralose FA_{cum}. Sucralose (●) is negative control, expecting lowest cumulative fraction diffused. ab = apical to basolateral transfer. n = 1. **(b)** Effect of increasing concentrations C10 on P_{app}. Note that no standard deviation can be shown for FA_{cum} or P_{app} as only one sample, for each concentration, was measured.

4. Discussion

The objective of this study was to investigate if there is a correlation between increased TJ permeability of the intestinal epithelium and absorption of obesogens and if obesogens alter the expression of intestinal TJs.

4.1 Transport of D-mannitol across obesogen exposed Caco-2 cell monolayers

Caco-2 cell monolayers exposed to BPA did not show change in D-mannitol transport. This was contrary to previously reported effects of BPA which have been shown to upregulate JAM-A [7]. Monolayers exposed to BPAF, especially low concentrations, showed reduced permeability. No previous findings can be used to compare this result to, but as the structure of BPAF is similar to that of BPA it is reasonable to believe that it can have similar effects. The pathway which BPAF acts on could then possible be the same as BPA where JAM-A and claudins are upregulated (Fig. 1), consequently reducing the paracellular permeability. Imi exposed monolayers showed increased permeability for some of the samples (Fig. 4c). Monolayers exposed to TBT-Cl showed reduced permeability for all concentrations of TBT-Cl. According to the pathway for TBT-Cl the reduction in permeability could be due to TBT-Cl acting on PPAR-γ and consequently increasing expression of tightening claudins proteins.

The results should, however, be taken with reservations since cultivation of cell monolayers experienced problems with leaking culture medium. The problem was especially frequent for the plate used for Imi and TBT-Cl tests. Similarly, the BPA and BPAF plates experienced this problem although not as frequently. However, the source of the problem was detected and solved, but the integrity of the monolayers could still be compromised due to lack of nutrients. In addition, only two monolayers were used for respective obesogen concentration. Furthermore, there could be additional error sources during performance of the organoborane sugar sensor method such as dissolving of 4,4'oBBV. There could also be mismatch errors with the sampling and labelling procedure.

For future studies, a positive control is a definite necessity to help further evaluation of the results from permeability tests. In addition, blank wells should be included to be able to evaluate the "resistance" that the cell monolayer provide against the permeability marker. The integrity of the cell monolayer is usually established with an epithelial volt/ohm meter for transepithelial electrical resistance (TEER). Since such equipment was not available and measurements could not be performed with a standard multimeter (which was attempted), monolayer integrity was assumed to be confluent after 21 days of culture. While considering that the result of D-mannitol permeation was very diverse, this could be due to compromised monolayer integrity or that the permeability marker solution was not homogeneous. In any case, the integrity should be better assessed in future permeability studies, favourably using an epithelial volt/ohm meter.

4.2 Effect of obesogens on tight junction protein expression

The great difference in protein concentrations could be due to numerous reasons, but the most probable one is that the same volume of lysis buffer, based on only one measurement of cell concentration, was added to each sample. Furthermore, it was noted during culturing that the individual monolayers differed in size, which could be a result of inequality during seeding and/or variance in toxicity of individual obesogens. Even so, no major differences in pellet sizes were noted.

The WBs could not be used to evaluate change in TJ protein expression as only incorrectly sized bands could be detected for BPA/BPAF (Fig. 8a) and Imi/TBT-Cl (Fig. 8c) exposed cells. This could be due to proteolysis or poor specificity of Abs. Another reason could be that the protein extraction was

insufficient resulting in limited yield of dissolved TJ proteins. However, the control, GAPDH, could be detected for both BPA/BPAF (Fig. 8b) and Imi/TBT-Cl (Fig. 8d) exposed cells. These images also illustrate that the background noise is much lower for GAPDH incubated membranes than with JAM-1, ZO-1 and claudin-2. This further indicated that there was a problem regarding specificity of either of the TJ Abs, which is discussed in section 4.4. The staining of SDS-PAGE gels revealed that only a limited amount of proteins remained in the gels for both BPA/BPAF (Fig. 9a) and Imi/TBT-Cl (Fig. 9c) exposed cells. However, the staining of the respective membranes also showed limited amount of protein (Fig. 9b and c), which could be a result of over-transfer or repeated stripping.

In summary, the WB method needs to be revised, especially at the protein extraction and protein transfer steps. Furthermore, different primary Abs should be applied if TJ proteins could still not be detected. With working protocol, one could proceed to study eventual change in TJ protein expression. This is done with densitometry calculation of the intensity of respective bands, which are normalised against the GAPDH control bands. A control, for change in TJ protein expression, should be included at the cell culture level to further support the study. In addition, this should be supported with a study of the TJ mRNA levels. Following this would be to further study the pathways of the individual obesogens. Antagonists could be used to target respective pathways the obesogens acts on, which should inhibit their effect on TJs. This could be studied using WB and comparing the results with or without antagonist. However, as obesogens have shown to target multiple pathways it could be difficult to prove that they act on specific pathways affecting TJs.

For future studies alternative methods such as *in-vitro* immunofluorescence may be used to directly visualize TJ proteins, which can make it more easily to study the protein expression. This could save time in comparison to the WB method as there are many more steps and each step may potentially be unsuccessful. In addition, such methods allow for direct study of the distribution of the TJ in the monolayer.

4.3 Epigenetic effects of obesogens on tight junction protein expression

The protein yields from cells exposed to obesogens (50 nM), were fairly low (Table 2). In addition, the concentrations were slightly lower than the observed concentrations from cells exposed to 10 nM (Table 1). This could be due to exposure to higher concentration of obesogens and/or the longer exposure time although no significant difference could be observed between 2 and 6 days. Hence, it is more likely a result of differences during the protein extraction processes.

The WB chemiluminescence images showed that TJ proteins could not be identified for BPA (Fig. 10a), BPAF (Fig. 10c), Imi (Fig. 11a) or TBT-Cl (Fig. 11c) exposed cells (including controls). Method optimization, including protein extraction, boiling time of protein extract, primary/secondary Ab concentration and diluents, WB transfer parameters, blocking buffer, blocking time and washing procedure, did not change the result. However, the background noise was reduced in comparison to the 10 nM exposed cells (Fig. 8), but with less success in stripping and reprobing with GAPDH primary Ab. With the reduce in background noise an evident signal was detected at 75 kD, but this signal did not match the actual size of any of the TJ proteins. Evaluating the primary Abs showed that the ZO-1 primary Ab was responsible for the signal, but it should show signal at 220 kD. This indicates a possible problem with primary Ab specificity and/or method of protein extraction and WB.

The protein transfers from samples exposed to BPA (Fig. 10a), BPAF (Fig. 10c), Imi (Fig. 11a) and TBT-Cl (Fig. 11c) were acceptable because no residual TJ proteins could be identified. There were residual large proteins (250 kD and above) for all transfers, but this was expected as large proteins transfers slowly. The residual small proteins (10 and 15 kD) for Imi and TBT-Cl is most likely due to the usage of a different blotting filter paper, which was not optimal for the WB transfer apparatus and

probably did not provide a uniform flow of buffer through the gel to the membrane. Furthermore, the staining of BPA (Fig. 12b), BPAF (Fig. 12d), Imi (Fig. 13b) and TBT-Cl (Fig. 13d) sample membranes showed possible traces of TJ proteins at ZO-1 (250 kD), JAM-A (37 kD) and claudin-2 (25 kD). However, the band at 37 kD is most likely GAPDH, while the 250 kD band is most likely another protein of that size and the 25 kD band may only be protein smear as the band is diffuse. On a further note, it has been reported that claudin-2 could not be detected in healthy sigmoid colon tissue, but was highly detectable in tissue with active Chron's disease [22]. Furthermore, the expression of claudin-2 has shown to be increased in patients with colorectal cancer [23]. Hence, this effect is likely to be seen in Caco-2 cells, but it is reasonable to retain the concept that they might not be expressed at detectable levels.

The epigenetic effect will have to be proven and studied further. There are various methods to study respective mechanism. DNA methylation of the promoter CpG islands of the TJs can for example be detected and assed by nucleic acid analysis. This can be achieved by bisulphite conversion of un-methylated cytosine, but not methylated, to uracil, following PCR and sequencing methods to identify and quantify the methylated cytosines [24]. Enriched histone modification, such as acetylation and methylation, can be analysed by chromatin immunoprecipitation methods where chromatin fragments, which carry specific modifications, is precipitated by the specific Ab. The purified DNA can then be subjugated to quantitative PCR and the enrichment of the target locus can be analysed [25]. The expression level of small, non-coding RNA can be studied with microarray analysis.

4.4 Evaluation of primary Abs

The evaluation of primary Abs showed that the ZO-1 Ab was responsible for incorrect signal at 75 kD and inducing high background noise (Fig. 14a). This was evident because no effective signal or background noise could be detected from JAM-A or claudin-2 Abs (Fig. 14b). These findings suggest that the ZO-1 Ab is non-specific, although the signal at 75 kD could be a result of partially degraded ZO-1 protein, but that is opposed by the high background noise and all the other bands that are obtained using the ZO-1 Ab. As for why no signal is obtained from JAM-A or claudin-2, this could be due to protein degradation or other reasons discussed earlier, such as problem with the yield and purity during protein extraction or the protein transfer method.

4.5 Transport of sucralose across C10 exposed monolayers

The obtained sucralose values were reasonable both for the apical and basolateral values compared to the theoretical starting concentration (Table 3). Further, analysis of CFT and P_{app} showed that Caco-2 cell monolayers exposed to 12, 35 and 108 mM of C10 increase the permeability of sucralose across monolayers (Fig 15). The result was in accordance to previous reported expected effect of C10 which suggests that $\geq$ 10 mM of C10 increase Caco-2 permeability [21]. Although these observations were only based on the data from single wells in a series of three replicates, they could still be used as a preliminary indicative effect of C10 on sucralose permeation. In any case, these findings suggest that C10 ($\geq$ 12 mM) impairs Caco-2 barrier functions, which allow for increased permeability of sucralose. This indicates that impaired IEB functions allow for increased permeation of molecules, which may or may not be harmful. As the sucralose obesogen permeated at an increased rate, it is most likely that other obesogens with similar structure and size act in the same way. The permeation of individual obesogens can be further quantified by applying other methods, such as liquid chromatography-tandem mass spectrometry techniques for BPA and Imi [26, 27] and gas chromatography for TBT-Cl [28]. The quantification of the obesogens and sucralose should also be performed on each well replicate to obtain a more accurate result. In addition, the study should be repeated with TEER measurements to ensure integrity of the monolayers at the start of the experiment.

4.6 Dot blots

The numerous dot blots performed in attempt to reduce background noise were fairly successful but could be further improved. The selection of membrane did not affect background noise (Fig. 7a – c). However, the selection of secondary Abs diluent did affect background noise since the buffer containing 3% BSA resulted in much higher background noise (Fig. 7d). This was not expected as BSA is commonly used for increased blocking of membranes. The reason could be due to contamination of the BSA resulting in cross-reactivity of the secondary Ab, although modern formulations are very pure. One of the types of weak interactions between antibodies and antigens is hydrophobicity. It is conceivable that hydrophobic interactions may occur between hydrophobic domains of Abs and one or both of the hydrophobic drug binding pockets of BSA. Ultimately, the dot blots aided to reduce the background noise, which was of aid to establish a working WB protocol. In this thesis, the limiting parameter was multiple bands at MW that could not unambiguously be correlated to the three TJ related proteins studied.

5. Acknowledgements

I would like to express my sincere gratitude to my supervisor Dominic-Luc Webb, co-supervisors Anas Al-Saffar and Abdul Halim, and the rest of the group at the Department of Medical Science Gastroenterology and Hepatology at Uppsala University Hospital for the great support during my master's thesis. Furthermore, I would like to thank my scientific reviewer Thomas Lind for all the great feedback during the project. Finally, I would like to thank neighbouring departments at Uppsala University Hospital for occasionally letting me borrow lab equipment.

6. References

1. Khan N, Asif AR. Transcriptional regulators of claudins in epithelial tight junctions. Mediators Inflamm [Internet]. 2015 [cited 16th June 2016]. doi: 10.1155/2015/219843

2. Ma Y, Semba S, Khan RI, Bochimoto H, Watanabe T, Fujiya M, Kohgo Y, Liu Y, Taniguchi T. Focal adhesion kinase regulates intestinal epithelial barrier function via redistribution of tight junction. Biochim Biophys Acta. 2013;1832(1):151-9.

3. Bischoff SC, Barbara G, Buurman W, Ockhuizen T, Schulzke JD, Serino M, Tilg H, Watson A, Wells JM. Intestinal permeability – a new target for disease prevention and therapy. BMC Gastroenterol. 2014;14(189).

4. Lee SH. Intestinal permeability regulation by tight junction: implication on inflammatory bowel diseases. Intest Res. 2015;13(1):11-8.

5. Grün F, Blumberg B. Environmental obesogens: Organotins and endocrine disruption via nuclear receptor signalling. Endocrinology. 2006;147(6 Suppl):S50-5.

6. Park Y, Kim Y, Kim J, Yoon KS, Clark J, Lee J, Park Y. Imidacloprid, a neonicotinoid insecticide, potentiates adipogenesis in 3T3-L1 adipocytes. J Agric Food Chem. 2013;61(1):255-9.

7. Braniste V, Jouault A, Gaultier E, Polizzi A, Buisson-Brenac C, Leveque M, G. Martin P, < Theodorou V, Fioramonti J, Eric Houdeau E. Impact of oral bisphenol A at reference doses on intestinal barrier function and sex differences after perinatal exposure in rats. Proc Natl Acad Sci. 2010;107(1):448–453

8. T. Schug T, Janesick A, Blumberg B, J. Heindel J. Endocrine disrupting chemicals and disease susceptibility. J Steroid Biochem Mol Biol. 2011;127(3-5):204–215.

9. Nilsson S, Mäkelä S, Treuter E, Tujague M, Thomsen J, Andersson G, Enmark E, Pettersson K, Warner M, Gustafsson JA. Mechanisms of estrogen action. Physiol Rev. 2001;81(4):1535-65.

10. Braniste V, Leveque M, Buisson-Brenac C, Bueno L, Fioramonti J, Houdeau E. Oestradiol decreases colonic permeability through oestrogen receptor β-mediated up-regulation of occluding and junctional adhesion molecule-A in epithelial cells. J Physiol. 2009;587(Pt 13):3317-28.

11. Boucher JG, Boudreau A, Atlas E. Bisphenol A induces differentiation of human preadipocytes in the absence of glucocorticoid and is inhibited by an estrogen-receptor antagonist. Nutr Diabetes [Internet]. 2014 [cited 16th June 2016]. doi: 10.1038/nutd.2013.43

12. Grün F, Watanabe H, Zamanian Z, Maeda L, Arima K, Cubacha R, Gardiner DM, Kanno J, Iguchi T, Blumberg B. Endocrine-disrupting organotin compounds are potent inducers of adipogenesis in vertebrates. Mol Endocrinol. 2006;20(9):2141-55.

13. Kinoshita M, Suzuki Y, Saito Y. Butyrate reduces colonic paracellular permeability by enhancing PPARgamma activation. Biochem Biophys Res Commun. 2002;293(2):827-31.

14. Ramakers JD, Verstege MI, Thuijls G, Te Velde AA, Mensink RP, Plat J. The PPAR-γ agonist rosiglitazone impairs colonic inflammation in mice with experimental colitis. J Clin Immunol. 2007;27(3):275-83.

15. Ogasawara N, Kojima T, Go M, Ohkuni T, Koizumi J, Kamekura R, Masaki T, Murata M, Tanaka S, Fuchimoto J, HImi T, Sawada N. PPAR-γ agonists upregulate the barrier function of tight junctions via a PKC pathway in human nasal epithelial cells. Pharmacol Res. 2010;61(6):489-98.

16. Heidrich DD, Steckelbroeck S, Klingmuller D. Inhibition of human cytochrome P450 aromatase activity by butyltins. Steroids. 2001;66(10):763-9.

17. Rezg R, El-Fazaa S, Gharbi N, Mornagui B. Bisphenol A and human chronic diseases: Current evidences, possible mechanisms, and future perspectives. Environ Int. 2014;64:83-90.

18. Kumar KK, Karnati S, Reddy MB, Chandramouli R. Caco-2 cell lines in drug discovery - an updated perspective. J Basic Clin Pharm. 2010;1(2):63-9.

19. Resendez A, Abdul Halim M, Landhage CM, Hellström PM, Singaram B, Webb DL.Rapid small intestinal permeability assay based on riboflavin and lactulose detected by bis-boronic acid appended benzyl viologens. Clin Chim Acta. 2015;439:115-21.

20. Scott H. Randell, M. Leslie Fulcher, editors. Epithelial cell culture protocols. New York City: Humana Press; 2013.

21. Lindmark T, Schipper N, Lazorová L, de Boer AG, Artursson P. Absorption enhancement in intestinal epithelial Caco-2 monolayers by sodium caprate: Assessment of molecular weight dependence and demonstration of transport routes. J Drug Target. 1998;5(3):215-23.

22. S Zeissig, N Bürgel, D Günzel, J Richter, J Mankertz, U Wahnschaffe, A J Kroesen, M Zeitz, M Fromm, and J-D Schulzke. Changes in expression and distribution of claudin 2, 5 and 8 lead to discontinuous tight junctions and barrier dysfunction in active Crohn's disease. Gut. 2007;56(1):61–72.

23. Dhawan P, Ahmad R, Chaturvedi R, Smith JJ, Midha R, Mittal MK, Krishnan M, Chen X, Eschrich S, Yeatman TJ, Harris RC, Washington MK, Wilson KT, Beauchamp RD, Singh AB. Claudin-2 expression increases tumorigenicity of colon cancer cells: Role of epidermal growth factor receptor activation. Oncogene. 2011;30(29):3234-47.

24. Osanai M, Murata M, Nishikiori N, Chiba H, Kojima T, Sawada N. Epigenetic silencing of occludin promotes tumorigenic and metastatic properties of cancer cells via modulations of unique sets of apoptosis-associated genes. Cancer Res. 2006;66(18):9125-33.

25. Kimura H. Histone modifications for human epigenome analysis. J Hum Genet. 2013;58:439–445.

26. Liao C, Kannan K. Determination of free and conjugated forms of bisphenol A in human urine and serum by liquid chromatography−tandem mass spectrometry. Environ Sci Technol. 2012;46(9):5003-9.

27. Taira K, Fujioka K, Aoyama Y. Qualitative Profiling and Quantification of Neonicotinoid Metabolites in Human Urine by Liquid Chromatography Coupled with Mass Spectrometry. PLoS One [Internet]. 2013;8(11). [cited 16th June 2016]. doi: 10.1371/journal.pone.0080332

28. Kannan K , Senthilkumar K, P. Giesy J. Occurrence of butyltin compounds in human blood. Environ. Sci. Technol.1999;33(10):1776–1779.

7. Supplementary data

7.1 Appendix A – Recovered D-mannitol mass

Table A1. Average D-mannitol mass from permeability test. The table show the average mass (mg) ± SEM calculated from concentrations (data not shown) from two replicate wells with four measurements per well. The theoretical mass of D-mannitol that was added was ~0.15 mg.

Sample	D-mannitol (mg)				
	Ap 0 min	Ap 30 min	Ap 60 min	Bas 30 min	Bas 60 min
BPA (nM)					
0 (Control)	0.177 ± 0.007		0.502 ± 0.012	0.188 ± 0.009	0.195 ± 0.006
0.1	0.188 ± 0.011		0.536 ± 0.011	0.203 ± 0.003	0.18 ± 0.003
1	0.173 ± 0.006		0.541 ± 0.015	0.198 ± 0.006	0.181 ± 0.007
10	0.158 ± 0.003		0.545 ± 0.01	0.191 ± 0.006	0.175 ± 0.006
100	0.168 ± 0.006		0.537 ± 0.006	0.196 ± 0.008	0.183 ± 0.007
1000	0.158 ± 0.007		0.54 ± 0.02	0.19 ± 0.004	0.177 ± 0.009
BPAF (nM)					
0 (Control)	0.177 ± 0.007		0.212 ± 0.004	0.174 ± 0.005	0.195 ± 0.006
0.1	0.208 ± 0.024		0.182 ± 0.004	0.129 ± 0.004	0.15 ± 0.007
1	0.181 ± 0.022		0.179 ± 0.004	0.122 ± 0.003	0.142 ± 0.006
10	0.164 ± 0.01		0.189 ± 0.004	0.124 ± 0.003	0.162 ± 0.008
100	0.154 ± 0.009		0.181 ± 0.004	0.128 ± 0.004	0.147 ± 0.006
1000	0.172 ± 0.008		0.175 ± 0.003	0.129 ± 0.005	0.134 ± 0.006
Imi (nM)					
0 (Control)	0.047 ± 0.005	0.107 ± 0.01	0.011 ± 0.003	0.035 ± 0.01	0.109 ± 0.003
0.1	0.207 ± 0.006	0.334 ± 0.014	0.241 ± 0.013	0.198 ± 0.015	0.14 ± 0.002
1	0.23 ± 0.015	0.328 ± 0.009	0.242 ± 0.016	0.187 ± 0.006	0.13 ± 0.003
10	0.23 ± 0.005	0.338 ± 0.015	0.238 ± 0.012	0.176 ± 0.009	0.127 ± 0.002
100	0.237 ± 0.015	0.356 ± 0.01	0.244 ± 0.011	0.168 ± 0.013	0.125 ± 0.003
1000	0.227 ± 0.009	0.321 ± 0.007	0.223 ± 0.015	0.195 ± 0.013	0.119 ± 0.001
TBT-Cl (nM)					
0 (Control)	0.047 ± 0.005	0.107 ± 0.01	0.011 ± 0.003	0.035 ± 0.01	0.109 ± 0.003
0.1	0.034 ± 0.004	0.048 ± 0.004	0.2 ± 0.014	0.008 ± 0.001	0.106 ± 0.003
1	0.043 ± 0.01	0.058 ± 0.004	0.195 ± 0.017	0.005 ± 0.001	0.107 ± 0.004
10	0.026 ± 0.002	0.044 ± 0.002	0.206 ± 0.014	0.007 ± 0.001	0.107 ± 0.003
100	0.029 ± 0.004	0.065 ± 0.007	0.184 ± 0.013	0.006 ± 0.001	0.099 ± 0.002
1000	0.027 ± 0.002	0.048 ± 0.005	0.18 ± 0.017	0.005 ± 0.001	0.108 ± 0.003

7.2 Appendix B – Percentage D-mannitol transported

Table B1. Percentage D-mannitol transported. Table show an approximation of percent D-mannitol transported from the apical side to the basolateral side after 30 min treatment with respective obesogen.

	% D-mannitol transported			
Obesogen conc. (nM)	BPA	BPAF	Imi	TBT-Cl
0	98	98	74	74
0.1	86	62	96	22
1	91	68	81	11
10	97	76	76	26
100	93	83	71	20
1000	96	75	86	18

7.3 Appendix C – FA_{cum} and P_{app} data

Table C1. Calculated FA_{cum} for sucralose transport. Nd = not detectable.

	FA_{cum} (cm)		
C10 (mM)	Sampling time (min)		
	20	40	60
0	0.690×10^{-2}	1.05×10^{-2}	1.50×10^{-2}
0.148	0.350×10^{-2}	0.528×10^{-2}	0.769×10^{-2}
0.444	Nd	0.366×10^{-2}	0.518×10^{-2}
1.33	Nd	0.384×10^{-2}	0.536×10^{-2}
4	Nd	0.383×10^{-2}	0.546×10^{-2}
12	0.642×10^{-2}	3.19×10^{-2}	4.00×10^{-2}
36	0.571×10^{-2}	1.51×10^{-2}	4.28×10^{-2}
108	0.939×10^{-2}	2.68×10^{-2}	4.43×10^{-2}

Table C2. Calculated P_{app} for sucralose transport.

C10 (mM)	P_{app} (cm/s)
0	4.05×10^{-6}
1.48E-01	2.07×10^{-6}
4.44E-01	1.60×10^{-6}
1.33E+00	1.66×10^{-6}
4	1.68×10^{-6}
12	1.21×10^{-5}
36	1.15×10^{-5}
108	1.25×10^{-5}